ABSTRACT

Scale Dependencies in Modeled Fire Behavior and Effects
in a Southern U.S. Grassland Ecosystem

Jian Yao, M.S.

Mentor: Joseph D. White, Ph.D.

FARSITE models were originally developed for the western grass and forests ecosystems thus predictive accuracy as a function of the scale of input data in southern grasslands is relatively unknown. To test predictive accuracy of the model in southern U.S grasslands ecosystem, two prescribed burns were conducted on the grasslands at Camp Swift, near Bastrop, TX. The spatial scale of FARSITE predicted fire behaviors and effects were assessed based on comparison of field observations and FARSITE simulations utilizing three different spatial resolutions of fuel map data.

The FARSITE simulations showed that, fine-scale fuel map derived simulation offered better area of burned prediction, better time of arrival simulation, and closer average temperature output. The time of arrival of fire simulation was less a scale dependence process than the temperature simulation. Prediction of fires in grasslands is limited by our detailed knowledge about mapping fine fuel loading, structure, contiguity, and interannual variability.

Scale Dependencies in Modeled Fire Behavior and Effects
in a Southern U.S. Grassland Ecosystem

by

Jian Yao, B.S.

A Thesis

Approved by the Biology Department

_____
Robert D. Doyle, Ph.D., Chairperson

Submitted to the Graduate Faculty of
Baylor University in Partial Fulfillment of the
Requirements for the Degree
of
Master of Science

Approved by the Thesis Committee

_____
Joseph D. White, Ph.D., Chairperson

_____
Darrell S. Vodopich, Ph.D.

_____
Sascha Usenko, Ph.D.

Accepted by the Graduate School
December 2009

_____
J. Larry Lyon, Ph.D., Dean

Page bearing signatures is kept on file in the Graduate School.

TABLE OF CONTENTS

LIST OF FIGURE

LIST OF TABLES

LIST OF GRAPHS

ACKNOWLEDGMENTS

I would like to acknowledgement my mentor, Dr. Joseph D. White from Baylor University, who originally developed the idea and provided basic planning and support for this project. I would also like to thank my other committee members, Dr. Darrell Vodopich and Dr. Sascha Usenko, for their support and scientific opinions on this project. I thank Jon Thomas for helping in the collection of data and field work. I also thank my colleagues in the Baylor Spatial Ecology Lab: Darrel Mary, Mary Sides, Zainab R. Naqvi.

I thank Texas Forest Service personnel, specifically Karen Ridenour who lead this project and also organized field work and prescribed burns, and provided fuel classification map, fire perimeter and field fuel data. I also thank Jennifer Korn, and Landon Temple from the Texas Forest Service for their assistance in collecting the data for this study. I thank to Rich Gray from the Texas Forest Service who safely conducted the prescribed burns of this study.

I would like to thank Texas National Guard personnel, Kate Crosthwaite, for offering the opportunity and support for this research.

I would also like to thank my family for supporting me study aboard. Also thanks for all my friends who helped me during this time. And finally, I thank my girlfriend, Shu Feng, for standing at my back throughout this entire process.

CHAPTER ONE

Introduction

Scale and Fire Modeling

Pattern and process probably are the two most important concepts in the ecology, and these two concepts both depend on scale. The space-time correspondence principle indicates that large-scale events tend to have slower rates and lower frequencies, whereas small-scale things are change faster and more frequently. For the purpose of scaling, levels of organization or integration are most useful when they are consistent with spatial and temporal scales.

Recognizing the appropriate spatial-temporal scale is important to landscape ecological analyses because this scale will influence the predictive power of landscape models (O'Neill, 1988). The complexity of an ecological model may be tightly linked to the spatial and temporal resolution of the data used for simulation (White and Running, 1994). Extrapolation from one scale to another scale can lead tends to errors if we do not clearly understand the underlying process of a phenomenon (Levin, 1992).

Fire atlases (fire perimeter data), topography, vegetation, and climate data can be integrated to study landscape-fire-climate relations and increase understanding of interactions among broad-scale ecosystem process (Rollins 2002). A standardized integrated approach was introduced for mapping fuels and fire regimes using extensive field sampling, remote sensing, ecosystem simulations, and biophysical gradient modeling to create predictive landscape maps of fuels and fire regimes (Rollins 2004).

Landscape Fire and Resource Management Planning Tools Project (LANDFIRE) is producing a comprehensive, consistent, scientifically credible suite of spatial data layers for the entire United States at the 30 meter resolution, which can be used to support landscape-level fire management planning. However, broad scale knowledge of landscape-fire-climate relations is largely based on extrapolations from finer scale fire study and application of data varies by locations and specific use (Rollins, 2009).

Because the factors that affect fire occur at different spatial and temporal scales, it is important to study the scale dependencies of fire prediction modeling. However, most of previous fire mapping researches was done in northern U.S forest land and the scales of research were relatively large in extent and in resolution (30 meter to 210 meter). Small scale fire researches that can offer additional information for the 30 meter resolution LANDFIRE project were rarely been conducted, especially in the southern U.S grasslands ecosystem.

It was thought that an "optimum" scale to fire modeling is the one that can preserve pertinent variability and without irrelevant detail. Research about choosing an appropriate resolution fuel map for fire modeling on semi-desert grassland/oak woodland indicates that the most appropriate scale for mapping fuels would be the one that characterizes the fuels to the finest spatial scale reflecting the heterogeneity of the fuel (Miller & Yool, 2002).

The primary object of the study was to study the fire behavior and effects modeling on the southern U.S grasslands fuel types. To reveal the scale effect in the model and the ecosystem, three kinds of cell resolution fuel maps derived from different remote sensing data with spatial resolutions that range from 1 to 30 meters were utilized

to model three prescribed burns. Two different spatial scale wind file were also used in the fire modeling.

Fire and Ecosystems

Grasslands Fire

Fire is a dominant ecosystem disturbance worldwide (Morgan et al., 2001) and affects succession through selection, regulates regenerating of plants, maintains biodiversity, and entrains ecosystem and biogeochemical processes at multiple scales (Rollins et al., 2004). The majority of fires occurring in grasslands, savannahs and woodlands are primarily supported by the herbaceous fuel load (in which grass species dominate), whereas the living trees typically do not burn (Smith, 2005). Global grasslands are typically disturbed by fire with return intervals of two to five years under natural conditions (Wessman et al., 1997). In grasslands, fire affects the vegetation community by suppressing woody growth, removing excess buildup of litter fuel, and stimulating herbaceous production. For example, annual burning can convert a wooded landscape to a fire-maintained grassland ecosystem (Bean et al., 2008). In another example, the absence of fire in mountain big sagebrush and grasslands in southwestern Montana make the area likely to become more homogeneous as Douglas-fir trees encroach (Heyerdahl, 2006). Study indicated that native tallgrass prairie can be converted to closed-canopy red cedar (*Juniperus virginiana*) forest in as little as 40 years in northeast U.S (Briggs, 2002).

Grasslands are the most common vegetation type in the United States, especially in the southern United States. In Texas, grasslands are found in seven biogeography

regions, including: (1) the Blackland Prairies (including the Grand, San Antonio, and Fayette), (2) the Coastal Prairie (including the Sand Plain), (3) the Rolling Plains (including the Rolling Red Prairie), (4) the Edwards Plateau, (5) the High Plains, (6) the South Texas Plains, and (7) the Trans-Pecos (David, 1985). In Texas, there are more than 570 grass species, among which 470 are native, leads the United States in the diversity of grass species (Diamond, 1985).

Before European settlement, fire was a natural ecological factor on the southern plains, and was considered to have maintained the grasslands diversity. Frequency of fire appeared to be highly variable and ranged from 5-30 years (Wright & Bailey, 1982). Following European settlement, suppression of fire combined with heavy livestock grazing has led to a gradual encroachment of woodlands into grasslands throughout southern Texas. Warm-temperate grasslands and savannas, typical of many landscapes in southwestern North America at the time of European settlement, have been replaced by shrublands and woodlands (Grant and Hamilton, 1999). Similar changes have been reported for Africa, India, Australia, and South America. In many of the world's dry lands, human-induced alteration of grazing and fire regimes over the past century has promoted the replacement of grasses by woody vegetation (Hibbard, 2003).

Over the past century, trees have encroached into grass- and shrublands across western North America (Heyerdahl & Miller, 2006). The immediate effect of losing grass cover is increasing the amount of bare ground. The long-term effect is soil loss through erosion, which reduces the capability of the land to support vegetation and permanently decreases the carrying capacity of the land for livestock and wildlife. Frequent, low-intensity fires maintain open grasslands by increasing mortality of trees,

particularly seedlings, saplings, and species with thin bark (Hessburg, 2005). Many of the native plant communities have evolved with periodic fires as a natural part of their life cycles. Eastern red cedar, an invasive woody species to southeastern United States, could be eliminated by frequent nature fires (USFWS). Beginning in the mid-twentieth century, south Texas land owners began to convert thorny woodlands back to grasslands in order to enhance rangelands for livestock production (Hanselka, 2007). The use of prescribed burns can initiate regeneration of these rangelands. As a result, there is an increasing interest in studying the fire behavior and effect in grasslands ecosystem.

Fire Behavior and Effects

The likelihood of fire in wildland is determined by weather, including precipitation amount, relative humidity, lightning occurrence, air temperature, wind, as well as fuel moisture/flammability (Pyne et al., 1996). Some scientists believe that the increased fire potential can be explained by understanding of fire-climate-vegetation linkages and the role of climate change, fuel buildup and land use activities in past fires. A study showed a consistent increase in regional-scale fire risk over Australia driven principally by warming and reductions in relative humidity as the climate change (Pitman, 2007). Higher spring and summer temperatures and earlier snowmelt are extending the wildfire season and increasing the intensity of wildfires in the western United States (Running, 2006).

The prediction of fire behavior is valuable for planning prescribed burns and for assessing potential fire damage to resources and ecological impacts. Factors influence the ignition and growth of wildfires have been very well studied (Finney, 1996 & 1998;

Whelan, 1995; Scott, 2005). Fire development and spread are related to fuel abundance and connectivity, soil and vegetation moisture, and weather and climate patterns.

The nature of the vegetation, along with the prevailing local climatic conditions, influences ignition by determining the amount of fuel available, flammability, and continuity of burnable surfaces. Ignition may occur when relative humidity is low, ambient temperature is high and fuel is dry. Climate affects the fuel moisture condition by curing fuel enough for combustion. Cold, moist fuels burn slower than hot, dry fuels. During the fire, moisture content in the air also affects temperature and fire behavior.

Wind is one of the most important environment factors that affect fire intensity and spread. It supplies oxygen to the burning fire front and increases the rate of combustion. Wind can also pre-heat the fuel through advection and increase the rate of spread of fire. In addition, in the absence of other constraints, a fire can generate its own wind (Whelan, 1995). Fire moves primarily along the wind direction as long as fuel is suitable.

Topography has similar influences as wind on fire behavior (Whelan, 1995). For an uphill fire, the topography makes flames stay closer to the ground and therefore pre-heat more fuels ahead of fire front. So, an uphill fire usually moves faster than a downhill fire. Valleys can generate "chimney" affect in a fire, and dramatically increase fire movement. Topographic features can also create firebreaks and thereby influence the distribution and spread of fire. Another major effect of topography is its interaction with local climate and the patch of plant communities. Regional wind pattern can change under the influence of local topographic as well as vegetation cover features, and create a local scale dynamic pattern.

There are three basic types of fires: surface, ground, and canopy (crown) fires. Each fire burns differently depending on the kind of fuel present. A surface fire burns fuels that are on the ground, as well as shrubs and trees. Small size and dry fuels cause a fast moving fire. Grass fires generally produce lower temperatures and burn quickly. If a fire burn fast, but without much intensity, the soil and trees are often not damaged. Surface fires can help keep surface fuels from building up and stimulate herb and shrub regrowth. A ground fire can occur when the duff layer becomes very dry. Duff is the organic layer of the soil consisting of decaying leaves and other plant parts, dead branches, and wood. A ground fire can creep slowly through the duff. It not only burns the dead leaves and wood, but can also burn the roots of living trees and plants. A canopy (crown) fire burns the higher leaves and branches of trees and shrubs, moves from tree to tree through the treetops. For a surface or ground fire, ladder fuels are required in order to move the fire to canopy.

The intensity of fire directly determines the fire influence on local environment. The effective radiation temperature of the fire front and the total energy released per unit area are important variables to estimate fire intensity (Rothermel and Deeming, 1980). These two variables both strongly correlate with the post-fire ecology of the sites. The temperature of the fire front is closely related to the survival rate of the living cells after fire. The total energy released per unit area is a measurement of the completeness of combustion. Ecological studies on the effects of fire rarely attempted to quantify fire characteristics, despite the obvious importance of fire behavior for survival of organisms and functioning of ecosystems (Whelan, 1995).

Fuels

The amount of energy stored in the fuel is an important predictor of fire intensity. Fuel load (total dry weight of fuel per unit of surface area), fuel moisture content, surface-area-to-volume ratio of fuel, and fuel depth are readily available indicators to describe fuel. Fuels were classified into three categories by which they respond to changes in moisture: 1 hour, 10 hour, and 100 hour fuels. 1 hour fuels are those fuel take approximately one hour to reach the same moisture level as environment, and usually are less than 0.6 cm in diameter. The diameter of 10 hour fuels range from 0.6 cm to 2.5 cm, and 100 hour fuels' diameter are between 2.5 cm and 7.8 cm. The collections of fuel properties have become known as fuel models and can be organized into four groups: grasses, brush, timber, and slash (Anderson, 1982). The measurement of fuel load and its effect on fire depend greatly on the type of fuel group. Rothermel (1972) and Albini (1976) tabulated 13 main fuel models for fire behavior predictions and applications.

Accurate estimations of aboveground dry biomass weight and moisture content are crucial to predicting fire behavior. There is a strong positive relationship between fuel load and fire intensity (Anderson, 1982). Fuel load indicates how much materials would burn during the fire and how much energy the fire will release. However, few fires can actually achieve complete combustion of the all above-ground biomass. When fuel load was measured, it is important to separate live fuel from dead fuel as they have different characteristics with regard to fire.

Fuel moisture content indicates how easy the fuel can be pre-heated and ready to burn. Moisture absorbs heat released during combustion, making less heat available to preheat fuel particles to ignition (Burgan and Rothermel 1984). Low moisture content

fuel is much easier to burn and burns faster than those fuels with high moisture content. At high moisture contents, the heat required to evaporate moisture in fuels is more than the amount of heat available in the firebrand (Simard 1968, Miller 1994), and combustion can be stopped. The environment factors that determine the fuel moisture of a fuel particle are: topographic feature, air temperature, moisture content of the air, solar radiation, and rain fall. Surface area-to-volume ratio is another fuel property that best describes particle geometry and the relative dimensions of the fuel-complex elements (Fernandes et al., 1998). It is a critical parameter in fuel characterization (Anderson, 1970), as large surface area-to-volume ratios increase the rates of energy and mass exchange with the gaseous phase, leading to lower ignition delays and higher rates of fire spread (Chandler et al., 1983). Fuel depth is also an important parameter involve in determining the packing density of fuel. While the packing density of fuel relates to how much oxygen is available for certain amount of fuel per unit area.

Most of lands are not covered by homogeneous vegetation type. As plant communities vary in their flammability, this affects the predicted rate of spread of fire. Less flammable plant communities can slow the rate of spread and serve as a firebreak in the same way as topographic features do. Fuel continuity plays an important part in determining whether a fire will spread (Whelan, 1995). Fuel continuity can be divided into two types: horizontal fuel continuity and vertical fuel continuity. Fuel continuity is necessary to allow fire to spread laterally across a surface, and through or into crowns. Surface fuel discontinuities act as barriers to fire spread under most conditions. Fire can burn rapidly and easily through the grasslands and sedge lands but less easily through

woodland patches. This difference can be explained partially by fuel continuity differences.

Remote Sensing

Remote sensing has been used to determine either fuel loading and/or fuel surface moisture conditions prior to the fire (Dasgupta et al 2006). The remote sensing data provides details on spatial heterogeneity that can be used as the input data for fire modeling. There are many remote sensing data available to be used to develop fuel map for fire modeling, and they all have their own characteristics. Three different resolution remote sensing data involved in this study are used to better understand the influence of grain size on input fuel maps for accuracy in fire modeling.

High resolution fuel maps can improve the accuracy of fire behavior modeling (Finney & Ryan, 1995). There were only a few published papers (Miller & Yool 2002; Rollins 2002) that have compared results of fires modeled with fuels mapped at different scales. This study tried to reveal the importance of fuel map scale effects on FARSITE modeling, in order to provide land managers with knowledge on which kind of scale fuel maps can be used to get accurate fire behavior simulations when working on grasslands fire in the southern United States.

DOQ Data

The Digital Orthophoto Quadrangle (DOQ) data are produced by the U.S. Geological Survey (USGS) and are gray scale, natural color, or color infrared (CIR) images with 1m × 1m ground resolution. The DOQ data used in this project were obtained from the TNRIS (Texas Natural Resource Information System;

http://www.tnris.state.tx.us/) and taken in July, 2004. The DOQ data contains three spectral bands which sample the green, red, and near-infrared wavelengths.

ASTER Data

The ASTER (Advanced Spaceborne Thermal Emission and Reflection Radiometer) provides high-resolution images of the Earth in 14 different bands of the electromagnetic spectrum, ranging from visible to thermal infrared. The resolution of images ranges between 15 and 90 meters. The ASTER data used in this project were downloaded from the Mid-American Geospatial Information Center (MAGIC) (http://synergyx.tacc.utexas.edu/). The latest data covering the study area was taken on May 22, 2005. To assess the fine fuels, data from the VNIR detector subsystem of ASTER were utilized, which has three spectral bands in the visible and near-infrared wavelength region with a spatial resolution of 15m × 15m.

Landsat 7 ETM +

Landsat 7 Enhanced Thematic Mapper Plus (ETM+) has the 30m × 30m spatial resolution on red and near-infrared wavelength region and the thermal infrared band 6 has 60m×60m spatial resolution. Data of Landsat 7 ETM+ for the study sites were downloaded from http://glovis.usgs.gov/ImgViewer. The date of this data taken was October 25, 2001.

The Normalized Difference Vegetation Index (NDVI)

The normalized difference vegetation index (NDVI), a simple numerical indicator of the live green vegetation (White et al., 1997), is used as an indicator of the vegetation condition. Live green plants absorb solar radiation in the photosynthetic active radiation

(PAR) spectral region, and use them as a source of energy in the process of photosynthesis. Leaves also tend to scatter and reflect solar radiation in the near-infrared spectral region. Hence, live green plants appear relatively dark in the PAR and relatively bright in the near-infrared regions of the electromagnetic spectrum. The NDVI indicates the difference of radiation in near-infrared and red wavelength (Equation 1).

$$NDVI = (NIR - Red) / (NIR + Red) \quad \text{Equation 1}$$

where Red and NIR stand for the spectral reflectance measurements acquired in red and near-infrared regions, respectively.

FARSITE Model

The FARSITE (Fire Area Simulator) model (Finney, 1996) used in this study has become a widely used fire behavior model by public land management agencies in the United States (Keane et al., 2000). FARSITE is a two-dimensional deterministic fire growth model that runs in a PC environment. The simulator incorporates existing fire behavior models of surface fire spread, crown fire spread, spotting, point-source fire acceleration and fuel moisture. FARSITE had been validated in conifer forest fires in Yellowstone and Glacier National Parks (Finney, 1993), and in Sequoia National Park (Finney, 1995), but has not been utilized in the southern United States grassland ecosystems.

The surface fire spread model used in FARSITE is the Rothermel spread equation (Albini 1976; Rothermel 1972) (Equation 2). It computes the steady-state fire spread rate (m min^{-1}) in a plane parallel with the ground surface at every vertex:

$$R = \frac{h\omega\gamma_s i(1+\Phi_w+\Phi_s)}{12.6\rho_b a_h Q_{ig}}$$ Equation 2

where R is the heading fire spread rate (m min^{-1}), h is the heat yield of fuel (kJ.Kg^{-1}), w is the weight of fuel per unit area (kg m^{-2}), r is the characteristic surface area to volume ratio of fuel bed (m^{-1}), i is the propagating flux ratio; P_b is oven dry bulk density(kg m^{-1}), a_h is the demensionless effective heating number, Q_{ig} is the heat of pre-ignition (kJ kg^{-1}), and Φw and Φs are wind and slope coefficient respectively. In this equation, h, w, r, i, ρ_b, a_h, and Q_{ig} are specific to different fuel types with values derived from laboratory analyses.

The wind and slope coefficients characterize the impact of local environment on the fire spread rate and are highly dependent on the characteristics of the surface fuel bed. Simplifying the equation showed the rate of spread is mainly determined by the fuel bed depth which is demonstrated in this study.

CHAPTER TWO

Methods

Site Description

Camp Swift Military Reservation is an Army training base managed by the Texas National Guard (TXARNG) and is located in the south-central portion of Texas (30°11′2″N, 97°17′52″W) in Bastrop County, approximately 35 kilometers east of the city of Austin, Texas. The property comprises 4750 hectares of area in the Colorado River basin. A comprehensive Integrated Natural Resource Management Plan for Camp Swift has being developed by TXARNG's Environmental Resources Management Branch (ERMB). The goal is to return lands to their original sustainable conditions by using prescribed-burns and restoration of native plant species.

Little blue stem (*Schizachyrium scoparium*) is a common North American prairie grass and is the dominant grass and main fuel in the open grasslands of the study site. It is a warm-season species and employs the C_4 photosynthetic pathway. Other herbaceous species in this area include partridge pea (*Chamaechrista fasciculata*), goldenrod (*Solidago virgaurea*), mustang grape (*Vitis mustangensis*). Mustang grape usually climbs woody plants, creating ladder fuels for fire spread. There are some woody species in the study area, including post oak (*Quercus stellata*), eastern red cedar (*Juniperus virginiana*), loblolly pine (*Pinus taeda*), yaupon (*Ilex vomitoria*), and Mexican plum (*Prunus mexicana*).

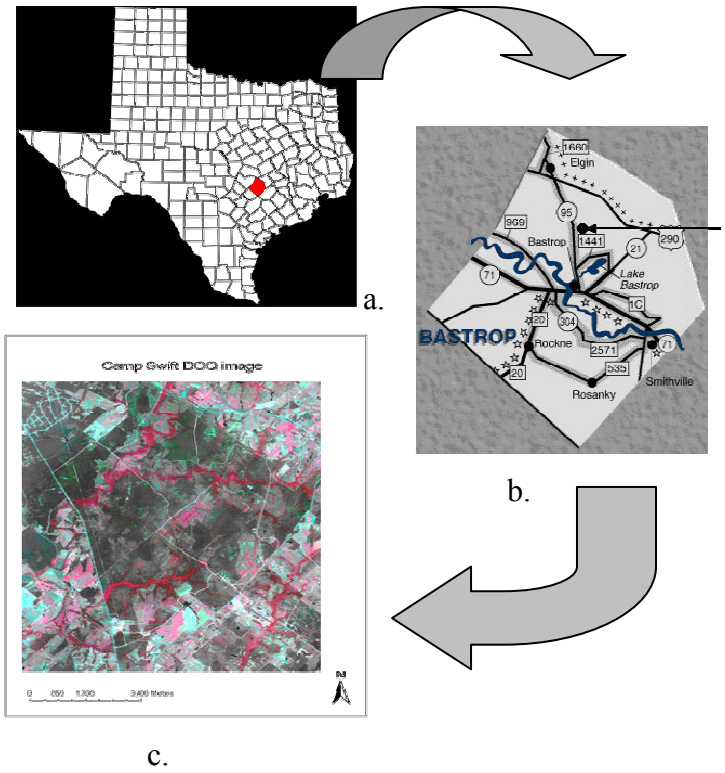

Figure 1. Map of study area. a. The map of Texas; b. The map of Bastrop County; c. The DOQ image of the entire Camp Swift base

The climate of the Camp Swift area is classified as subtropical. Humid, tropical weather dominates during summer, and continental weather patterns dominate during the remainder of the year. The mean annual temperature is approximately 20 ^{o}C (68°F). January is the coldest month, with an average low temperature of approximately -6.4 ^{o}C (20.4°F), and August is the warmest, with an average high temperature up to 40.1 ^{o}C (104.2°F). Typically 22 days each year have temperatures of freezing or below. Temperature variations between night and day tend to be moderate during summer and winter with a difference that can reach 5 ^{o}C.

Measurements taken during the period 1900-1983 at the National Weather Service monitoring station in Smithville (approximately 20 kilometers southeast of Camp Swift)

indicated that precipitation averages about 93cm (36.7 inches) annually, with measurable precipitation (0.01 in. or more) falling on at least 82 days each year (Larkin & Bomar, 1983). Rainfall is fairly evenly distributed throughout the year. May has the highest average monthly precipitation at approximately 10 cm, and August has the lowest at just over 5 cm. Snow is rare in this area for the most years. Winds average about 14.5 km/hr and are mainly from the south. Winds of 80 km/hr occur about once every two years. Airborne dust occurs infrequently. Camp Swift area historical tornado activity was near Texas state average.

Two major soil associations dominate at the TXARNG property. There are the Patilo-Demona-Silstid association in the northern part of Camp Swift and the Axtell-Tabor association to the south (Baker, 1979). The Patilo-Demona-Silstid association has a sandy surface layer and moderately slowly permeable to moderately permeable lower layers. The hazard for erosion of these soils is slight to moderate (Avaklan et al., 1993). In the Camp Swift Reservation, Big Sandy Creek flows through an area dominated by the Patilo-Demona-Silstid group.

The topography of the Camp Swift area is gently rolling to undulating, and regionally the ground surface dips from northwest to southeast. Most of the TXARNG property is 135-155 meters m (450-500 ft) above the mean sea level (MSL); although the site elevation in the western portion of the property near State Highway 95 is as much as 180 meters (590 ft) above MSL.

Field Data

Pre-Fire

Three prescribed burns were conducted and analyzed at Camp Swift, referred to as Study Site 1, 9 and 10 (Figure 2).The Study Site 1 was located at the west side of Camp Swift and had 9 hectares of continuous open fuel bed covered mostly by tall grasses (little blue stem), with vegetation patches of partridge pea, mustang grape, and goldenrod ranging in size from 2000 to 8000 m^2 (0.5 to 2 acres). The north side of burn unit 1 was covered by a heavy woody boundary with creek under that; the west and south side of unit was open road with black already burned place beyond that. The unit was flat with an elevation of 50 meters (163 feet) above MSL. Previous prescribed burns were conducted on the Study Site 1 in February 2002 and January 2005. And, a wildfire happened on this area in June 2006. The Study sites 9 and 10 were close together and located at the east side of Camp Swift and at west side of Texas State Highway 290 with a combined area of approximately 20 hectares. These two units were also dominated by little blue stem and were separated by a heavy woody line. A large part of little blue stem area at the northern side of the Study Site 10 was mowed in the previous summer. The fuel was predominately new growth little blue stem and mustang grape. Within each study site, some fuel patches different from little bluestem were imbedded. The prescribed burn sites were surrounded by wooded boundaries dominated by post oak, loblolly pine, and yaupon. For the Study Site 10, a small elevation rise occurred across the burn unit ranging from 137 meters (450 feet) above MSL along the southern tree line to 160 meters (550 feet) above MSL to the observation area on the north side of the unit, with a slight south aspect. The Study Site 9 is relatively flat with an elevation of 134

meters above MSL on the south side of the burn unit rising to 135 meters at the north side of the burn unit. Previous prescribed burns were conducted on the units in December 2000 and February 2002.

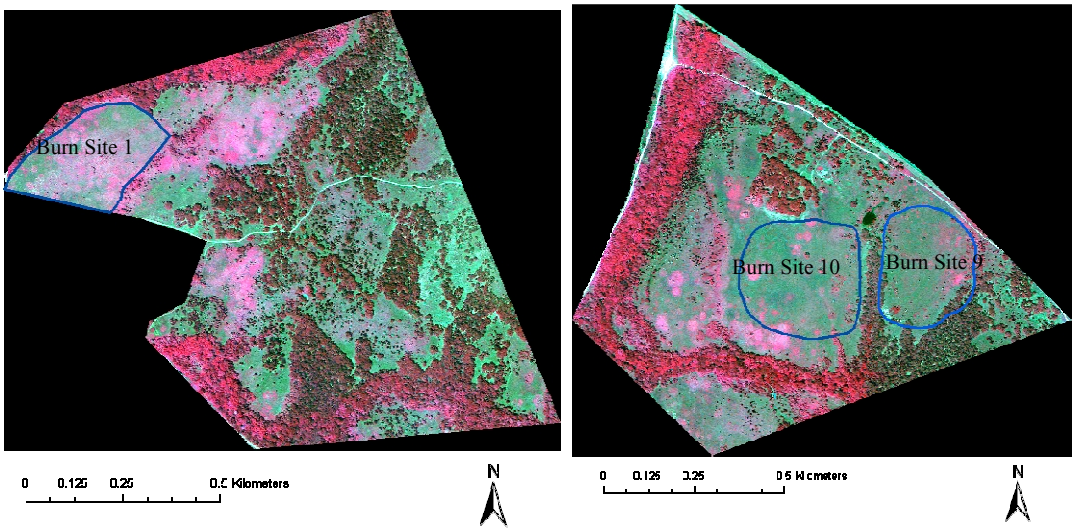

(a) Study site 1 (b) Study site 9 and 10

Figure 2. DOQ image of prescribed burn site. The blue polygons indicate the original prescribed burn area. The images show approximately the real fire burned area. In these images, red color represents near infra-red reflectance, green color indicates red, and blue color indicates green. (a.) study site 1; (b) study site 9 and 10.

In order to record prescribed fire behavior, data collection points were set up in each study site before the fire. There were 29 points for the Study Site 1, 24 points for the Study Site 9, and 34 points for the Study Site 10. Those data collection points were spread according to the shape of burn site and with a 30 meter interval between each other. The GPS coordinates of each data collection point were recorded and each point was marked by a 3 meter long pole. The fire data loggers were deployed at the east side of each pole to record the soil temperature change during the fire. The main components of fire data loggers were HOBO thermocouple loggers (Onset Computer Corporation, Bourne, Massachusetts). Three types of thermocouple loggers were currently available

with different temperature recorded ranges and resolutions: types K, J, and T. The type K loggers, which recorded temperature change in every five seconds, were used in this study. From the data recorded by fire dataloggers, some parameters of fire could be calculated (1) peak temperature, defined as the maximum value logged; (2) duration of heating, defined as the time over which temperatures exceed some predetermined baseline value; (3) total heating, defined as the sum of temperature values above baseline during a fire, measured in degree-minutes; (4) rate of spread, defined by the time lapse between peak temperatures at thermocouple junctions at known distances apart (Grace et al., 2005). The mean peak temperature of fire was thought to be a good indicator of energy released by fire. The mean peak temperatures were calculated from 12 recorded temperature values (1 minute of observation) recorded during the maximum temperature period (25 seconds before the maximum and 30 seconds after the maximum temperature occurred). The calculated mean peak temperatures of fire from the fire dataloggers were compared with simulated fire temperatures calculated from reaction intensity values output by the FARSITE model. The method of calculate fire temperature from model output reaction intensity is discussed later.

Fuel Loading, Aboveground Biomass

Fuel sampling was conducted at the west side of each data collection point poles as a part of a larger study on fire behavior in these grasslands conducted by the TNG and TFS. A 0.5 × 0.5 meter quadrat was used to constrain the area for clipping grass fuels with clipping conducted at 2 meters west to the data loggers in order to reduce influence on nearby fuel loading conditions. The grass fuels were not equally distributed within the vertical clone space of quadrat, and appear as two-phase distribution. The top part was

determined to be those above 35 cm to 40 cm, loose packed grass; the bottom part was the remaining materials except soil, usually dense packed with these phases depths identified visually and measured for each plot. All top and bottom grasses at each point were cut and collected into two separate bags. The clipping followed the same procedure in order to minimize individual bias.

Dead Fine Fuel Moisture Content

Accurate estimation of fuel moisture content is important for predicting ignition probability, fire behavior, and fire intensity. To measure the instant moisture content, we used the clip-and weight method. A branch of up and bottom fuels were clipped at each data collection point. The biomasses of samples were weighted immediately in the field to get the most accurate wet weight data. Then, the dry weight data were collected after placing the fuels in a drying oven under 65.5°C for 24 hours (unpublished data from Karen Kilgore, TFS). The formula used to calculate relative moisture content is RMC= [(Wet-Dry)/Dry] × 100. In the model, these values are averaged into a single starting value for 1-hour fuels for grass fuel.

Fuel Bed Depth and Fuel Patches Polygon

There is a strong positive relationship between height of scorch on the vegetation and fire line intensity (effective radiation temperature of the fire front) (Rothermel & Deeming, 1980). At each data collection point, fuel height (also called as fuel bed depth) and the fuel species were recorded, therefore.

Plant communities vary in their flammability for various reasons, such as the relative moisture, fuel type, fuel continuity and so on. Less-flammable plant

communities interspersed with more-flammable ones can act as firebreaks (fire will slow down when comes across less-flammable plant communities). A GPS unit was used to take record of large fuel patches and created fuel type polygons.

Surface Area-To-Volume Ratio

Surface area-to-volume ratio is a critical parameter in fuel characterization. Large surface area-to-volume ratios increase the rates of energy and mass exchange with the gaseous phase, leading to lower ignition delays and higher rates of spread (Chandler et al., 1983). Surface area-to-volume ratio plays a major role in fire modeling; thus, it must be quantified for accurate simulation. There were two methods used in this study to determine the SAV ratio.

The first method was developed from water immersion technique (Fernandes et al., 1998). The fuel samples were oven-dried for 24 h at 60° C. The dry weight (W_1, g) was measured first. Then, the fuel samples was handled with tweezers and maintained under water in a cylinder for five seconds. According to Archimedean law, the volume of fuel can be directly read as equal to the volume change of water (V, cm^3). Adhesion of air bubbles to fuels was prevented when reading the volume change. After the material was displaced from the water, it was necessary to remove some water in excess at its surface. To do that, the fuel piece was placed in a common household centrifugation device (a salad spinner) and rotated five times. Wet weights of fuel (W_2, g) were determined after the excess water been removed.

The final equation of water immersion technique to calculate surface area-to-volume ratio was:

$$\sigma = (W_2 - W_1)/ V \cdot t \qquad \text{Equation 3}$$

where σ represents surface area-to-volume ratio and t is the thickness of the adsorbed water pellicle (cm).

When a fuel particle was withdrawn from water after a previous immersion, a certain amount of liquid was absorbed to its surface. The volume of water was a function of particle surface area and thickness of the absorbed water pellicle (t, cm). The value of t was determined as 0.033 based on the study of Paulo (1998).

The other method was called modeled leaf and stem technique. There are two major parts of vegetation fuel: leaf and stem. In calculation of surface area-to-volume ratio, the shape of leaf was considered as regular cuboids with small height (like a paper), and the shape of fuel stem was assumed to be cylinder shape.

Equation 4 and 5 showed the calculation of surface and volume for leaf fuel. Equation 6 indicated the area-to-volume ratio of leaf was just a function of the thickness of leaf.

$$S_l = 2*a*b \qquad \text{Equation 4}$$

$$V_l = a*b*z \qquad \text{Equation 5}$$

$$SAV_{leaf} = 2/z \qquad \text{Equation 6}$$

where a is the long of leaf, b is the wide of leaf, and z is the thickness of leaf.

Equation 7 and 8 showed the calculation of surface and volume for stem fuel. Equation 9 indicated the area-to-volume ratio of stem was a function of radius and height of stem.

$$S_s=2\pi r^2+2\pi rh \quad \text{Equation 7}$$

$$V_s=\pi r^2 h \quad \text{Equation 8}$$

$$SAV_{stem}=2/h+2/r \quad \text{Equation 9}$$

where r is radius of the stem, h is height of stem.

The leaves and stems of individual samples were separated and used caliper to measure the thickness of leaf, the diameter and height of stem. The SAV value for leaf and stem can then be calculated by equation 5, 8. To get the combined surface area-to-volume ratio for each species, the average weight ratio of stem and leaf was assumed equal to the ratio of their surface area-to-volume ratio (Equation 10).

$$W_{leaf}/W_{stem} = SAV_{leaf} / SAV_{stem} \quad \text{Equation 10}$$

Prescribed Fire

The prescribed fires were primarily conducted by Texas Forest Service (TFS) fire crew with help from TXARNG, Baylor University personnel and other agencies. Standard prescribed fire procedures were followed in these study fires. Specific prescribed burn plans were set up according to each study site situation and weather condition at the time of burn (provided and conducted by TFS). The prescribed fires were conducted under the condition that all weather parameters were within acceptable weather condition ranges with wind speeds between 8-24 km/hr, the relative humidity between 20-50%, and the temperature between 24-35 °C. Single ignition method was used in the prescribed burn in order to simulate natural lighting-cause fire.

Photo shooting and video recording were taken during fires from several directions. Flame lengths of fire were estimated from char measured on 3 meter high poles at the each data logger point. Several Kestrel Pocket Weather Trackers (4500,

Nielsen-Kellerman Cop., Boothwyn, PA) were set around the burn sites to record the weather and wind changes. After the burn, the fire perimeters were mapped as polygons by using a recording GPS. And all the data loggers were recovered to download the data.

Fire Simulation & FARSITE Input and Output Data

Simulation of FARSITE required spatially landscape file (.LCP), temporally files liked weather (.WTR) and wind file (.WND), and fuel class specific parameter files liked custom fuel model file (.FMD), moisture file (.FMS) and adjustment file (.ADJ). Weather and winds were input into FARSITE model as streams of data, and wind data can also be input as raster spatial file. The fuel condition and topography data were input into landscape file as GIS raster themes.

Input Landscape File (.LCP)*

The landscape file included topographic information and fuel information. The topographic data included elevation, aspect, and slope raster. All these files were derived from a Triangulated Irregular Network (TIN) file of the Camp Swift. The TIN file was developed from the point elevation value data provided from Texas National Guards which were recorded by Light Detection and Ranging (LIDAR) sensor (Kate Crosthwaite, Texas National Guard, unpublished data). Road and other any types of burned or dozer areas were considered as barriers for fire movement, therefore, they all been constructed in the landscape file. All data were processed using ArcGIS 9.2 software with data input into FARSITE in ASCII format.

Fuel data in the landscape file contained fuel map, canopy cover, stand height, crown base height, and crown bulk density. The method of developing fuel map was

discussed later. Tree canopy cover was set as averagely 80%, tree canopy height was set as constant 10 meter, crown base height was set as 2 meter, and crown bulk density was defined as 0.2 kg/m^3. All these data were derived from a study conducted at the nearby Balcones Canyonlands National Wildlife Refuge (White, unpublished data).

Fuel Maps of Different Resolution

The fuel map used by FARSITE was a raster format file with individual cell assigned as a fuel type. Fuel maps were developed from different remote sensing data and input into FARSITE as a part of landscape file (*.LCP). Each fuel type on the fuel map related to a custom fuel model (*.FMD) that included parameters FARSITE depended on to simulate fire.

Data for DOQ, ASTER and Landsat ETM+ were input and processed using ERDAS IMAGINE 9.0 image software. All data were co-registered to a WGS84 datum in Universal Transverse Mercator (UTM) zone 14 and georeferenced according to the DOQ image to minimize variance. Finally, all images were subset to include only the burn sites.

In order to determine fuels from each of the remote sensing data source, an initial coarse level vegetation-type map developed from SPOT satellite data (Provided by Texas Forest Service) was used to mask the NDVI values for individual fuels model (Anderson, 1982). Next, the minimum, mean, and maximum NDVI value for each main fuel types were produced by statistical analysis using the image processing software (ERDAS). The minimum, mean, maximum NDVI values and their corresponding fuel loading values were then used to derived the least-squares linear regression models (y=mx+b) for each main fuel model where NDVI was the independent variable and fuel loading was the

dependent variable (Graph 1). The fuel loading value for fuel model 3 (Tall grass, FM3) was obtained from field measurement in the study area; while fuel loading values for fuel model 6 and 8 (Brush and litter) were derived from a study conducted at the nearby Balcones Canyonlands National Wildlife Refuge (White, unpublished data). The regression equations were produced by Microsoft Excel spread sheet. Subclasses of each main fuel type (e.g. tall grasses – FM3) were then determined by stratifying the fuel loading values based on the minimum-maximum fuel loading values calculated from NDVI value using regression equation. The stratify procedure were conducted by using the variation of field measured fuel loading values as the benchmark.

Input Metrological Data

Metrological data, including air temperature, fuel temperature, fuel moisture content, relative humidity, and wind speed and direction, were obtained from Remote Automated Weather Stations (RAWS) USA Climate Archive (http://www.raws.dri.edu/wraws/txF.html) and input into FARSITE as weather (.WTR) and wind (.WND) file. Instant wind speed and direction at the each burn site were also recorded by more than three Kestrel Pocket Weather Trackers.

Wind direction and speed are greatly influenced by the topographic features when it moves across the landscape, which might cause a significant result on fire behavior. WindNinja 1.0 (Rocky Mountain Research Station, Missoula Fire Sciences Lab) offers a way to calculate spatially varying wind caused by topographic variation on wildland. The vegetation above ground is considered have a similar affect on wind pattern change as the topographic feature does. However, this effect later had been confirmed relative

small in this project. So, the vegetation height was not included in the WindNinja calculation.

Input Custom Fuel Model File (.FMD)*

The custom fuel model file contained parameters that used to describe each fuel class, including the fuel loading, surface area-to-volume ratio, fuel bed depth (fuel height), the moisture of extinction, and the heat content. Parameters were pre-set before simulation. Those values were from references and field measured data, and were modified in the model calibration process.

Input Initial Fuel Moisture File (.FMS)*

Average relative moisture contents were assigned to each fuel classes before simulation by considering both field measured and reference values. During simulation, the fuel moistures were calculated using the model from Nelson (2000) through the simulation. FARSITE used the dead fuel moistures supplied as "initial fuel moistures" and modified them according to the changes in temperature, humidity, rainfall, cloud cover, and the local site topographic conditions. Live fuel moistures specified for a given surface fuel model remained constant throughout the entire simulation. The “condition period” function in FARSITE allows the model use preceding days’ weather conditions to calculate fuel moisture at the time of fire ignition. If the function not selected, the model would use pre-set input values from the initial fuel moisture file as the ignition moisture. The simulations were run without “condition period” function and used the pre-set fuel moisture values as the initial moisture. Two initial fuel moisture files were created for both winter and summer burn scenarios, individually.

Input Adjustments File (.ADJ)*

An adjustment factor file in the FARSITE model allows the user to use recorded data to tune the simulation to observed condition. Factors in adjustment file are fuel class specific and are multiplied by the rate of spread to achieve the specified adjustment. During modeling calibration and confirmation, it was found that adjustment factors were necessary to achieve most accurate fire modeling results with results described later.

Output Data

The extents and configurations of the simulated fire area were considered as the first parameter to evaluate fire simulation accuracy. The simulated final fire perimeters were output from the FARSITE, and were compared with the GPS recorded real prescribed fire perimeters. The times of arrival of fire indicated the spread rate of fire and were an important parameter in fire management. The time of arrival of simulated fire were output from FARSITE as raster files, with each pixel of file assigned with an arrival time value. The TOA files were processed in ArcGIS software. The extracted simulated TOA values at each datalogger were compared with the recorded TOA values.

The reaction intensity was considered as an indicator of fire impact on local environment and was very important for post fire ecology. Reaction intensity in FARSITE model was calculated by estimating the consuming rate of fuel and the amount of heat yield per unit fuel. The fire temperatures can be calculated from the simulated reaction intensity, and then compared with temperatures recorded by dataloggers.

The Stefan–Boltzmann law was employed to calculate temperatures from the reaction intensity (kW m^{-2}) values derived from the simulation. The Stefan–Boltzmann law states that the total energy (kW m^{-2}) radiated per unit surface area of a black body in

unit time is directly proportional to the fourth power of the black body's thermodynamic temperature T:

$$M_{\lambda} = \varepsilon \sigma T^4 \qquad \text{Equation 11}$$

where M was the reaction intensity; T was the temperature; σ was the Stefan–Boltzmann constant, which equal to 5.67×10^{-8} $Js^{-1}m^{-2}K^{-4}$, ε was the emissivity.

Model Initialization, Calibration, and Confirmation

The model was applied to the three prescribed burns at Camp Swift, Elgin, Texas. For initializing simulations, meteorological, topographic, and fuel condition (fuel loading, moisture, surface area-to-volume ratio, height) data were required. Fuel data were sampled from field and modified for each fuel class in the input custom fuel model file. Based on the parameters Anderson (1984) offered for his basic main fuel models, as well as sampled fuel data in this study, multiple characteristic parameters for different fuel types, upon which FARSITE model depended to simulate fire behavior, were modified in order to fit the model in the grassland fire scenarios. As an initial estimation of the model prediction, a perimeter of the burn was collected by Texas Forest Service personnel immediately following both fires. Two aspects of FARSITE calibration were done based on study site 1 burn data: 1) fire extent and configuration and 2) time of arrival. The calibration was done by changing the parameters values and modifying the adjustment factors for each fuel class.

The calibration of the model was firstly conducted on the Study Site 1 (winter burn), and yield the best-known fuel parameters (See Results Section 3.4). The model then been applied on the Study Site 10 (summer burn) with some modifications in

adjustment file in order to accommodate the seasonal scenario variation. The model was finally confirmed on the Study Site 9 (summer burn).

Analysis of Scale Effect and Simulation Accuracy Assessment

Three scale analyses of FARSITE modeling were completed in this study. The first was the scale effect of fuel model. Anderson's 13 main fuel models were considered not sufficient for small scale FARSITE simulation. Fuel maps contained sub-fuel classes other than just the main fuel models were developed. The effect of developing sub-fuel classes was analyzed by comparing simulation results from using main fuel model only with the ones using sub-fuel classes. The second scale effect was the effect of fuel map resolution. Three remote sensing data were used to derive different resolution fuel maps. The simulation results from all three scale fuel maps were analyzed. The last tested scale effect was the spatial scale effect of wind data. The spatial variance wind pattern files, created by WindNinja software, took the effect of changing topographic features on wind pattern into account. The results from simulation with fine scale spatial variation winds were compared with those results come from simulations only using average general wind speed and direction.

Three major indictors were included in the results analyses: the final extent and configuration of fire area, the time of arrival of fire, and the temperature yield by fire. Fire extent was the primary indicator of the accuracy of a fire model. For the comparison of fire area, the null hypothesis was the simulated fire burned area was not significantly different from the real fire. Error matrix, the most common way to represent the accuracy of a remote sensing vegetation type classification (Congalton, 1983), was used to compare the burned and unburned area of real fire with the simulation fire. An error

matrix is a square array of numbers set out in rows and columns, with reference data (i.e., real burn data) represented in columns and simulated data indicated in rows. Because the values on the major diagonal represented those pixels that had been correctly classified, the overall accuracy of error matrix was the sum of these values divided by the total number of pixels. The Kappa statistics (K) were calculated from the matrices as a measure of accuracy of agreement (Equation 12) (Landis and Koch, 1977).

$$\hat{K} = \frac{N\sum_{i=1}^{r} x_{ii} - \sum_{i=1}^{r}(x_{i+} * x_{+i})}{N^2 - \sum_{i=1}^{r}(x_{i+} * x_{+i})} \qquad \text{Equation 12}$$

where r is the number of rows in the matrix, x_{ii} is the number of observations in row i and column i, x_{i+} and x_{+i} are the marginal totals of row i and column i, respectively, and N is the total number of observations (Bishop, 1975).

The time of arrival of fire was also an important indicator for fire behavior prediction. In term of time of arrival, FARSITE revealed information that when fire arrived at certain point, which was especially important for fire fighters as it informs them of potentially dangerous conditions. For the time of arrival comparison, a least square regression model was used to determine whether there was significant linear relationship between the recorded data and simulated data. There are four statistic parameters were calculated for the regression model and were used to judge the accuracy of model: standard error (SEE), correlation coefficient (r^2), slope, and intercept. The standard error (SEE) and correlation coefficient (r^2) indicated whether the model "work" (the fidelity of the model). And the slope and intercept showed the level of accuracy of

the model. All the values of 4 parameters were tested significance at 0.05 α level (SPSS, 13.0).

Finally, the temperature yield by fire was an important parameter for fire intensity analyses and post-fire ecology study. Analyses of temperature were similar to the analyses of time of arrival. The average temperatures from each simulation also were compared.

CHAPTER THREE

Results

Prescribed Fires

The first prescribed burn was conducted on January 10, 2008 at the 9 hectare large Study Site 1. The average air temperature at the burn date was lower than 15°C, relative humidity was less than 35 % and average wind speed was 4 m/s (9mph) according to the RAWS data. The ignition point for Burn 1 was at the northeast corner of the original prescribed field (Figure3, a). The wind changed to the northwest from the predicted northeast direction just after the ignition at 12:52 pm local time. As a result, fire burned toward the east and moved into the east side forest line 15 minutes after the ignition. Only the flank of fire slowly burned across the originally prescribed field, while the head of the fire was driven by the wind to the southeast direction and beyond the original prescribed area. It took three hours for the fire to consume the original 8 hectare area, and total burn area reached almost 43 ha in 4 hours (Figure 3, a). Fire behavior, such as the rate of spread and the condition of smoke, changed when the fire came across fuel patches like partridge pea, mustang grape, and goldenrod. Heavy load wet fuel, like mustang grape and goldenrod, was hard to ignite and acted as fire breaks. Fire burned slowly and with low intensity on those patches. Shrubs like patches (e.g. partridge pea) were slowly ignited but created high intensity fire. Flame height averaged 7 meter high and varied between 3 to 13 meters. There was no crown fire activity during this burn.

The second prescribed fire was conducted on July 18, 2008 at the Study Sites 9 and 10. The average air temperature at that day was 30°C, relative humidity was 42%, and average wind speed was 2.4 m/s. The Study Site 9 and 10 were originally planned to burn separately, and a black line was set between two study sites to restrict fire. The single fire consumed both the study sites due to the fire jump. The original ignition point was at the south corner of the Study Site 10 at 13:07 local time (Figure 3, b). The fire burned 10 hectares of the Study Site 10 within one and an half hour. And then, the fire moved past the black line and consumed 8 hectares of the Study Site 9 in two hours. Flame heights were low in the mowed area, but went up higher to average 10 m when the fire hit un-mowed tall grass. Fire consumed parts of forest line around both study sites, and severe crown fire activities were observed.

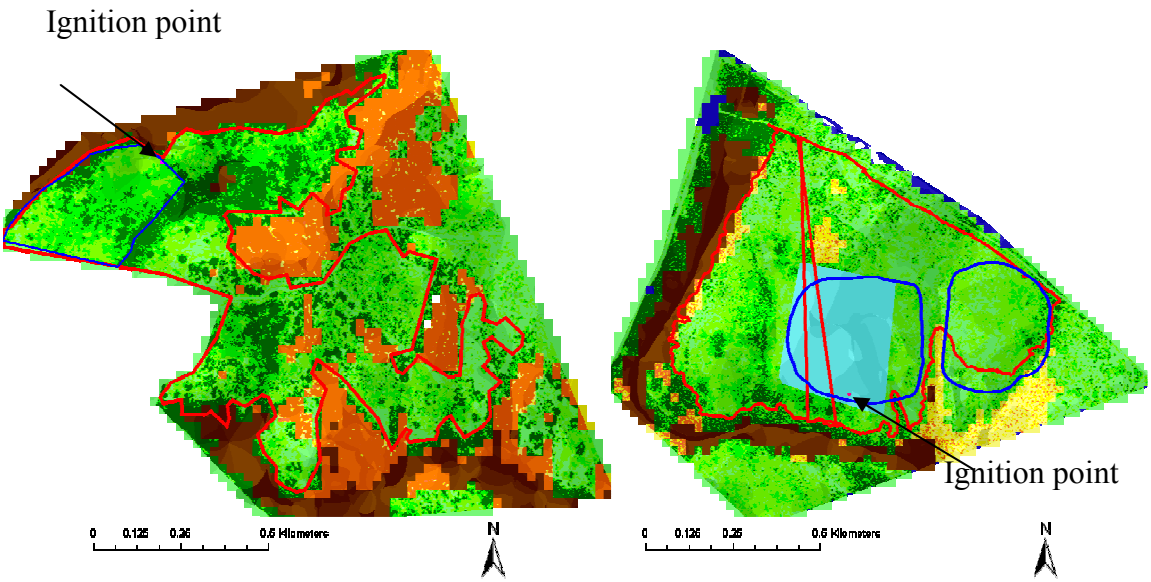

a. Study site 1 b. Study site 9 & 10

Figure 3. The developed fuel map from DOQ data. The pink dots indicate the ignition point; the red bold lines represent real fire perimeter; the blue bold lines represent the original prescribed burn area. Different colors on the map represent different fuel types: green indicates grass fuel (FM3, the darker the color is, the heavier the fuel loading is); yellow to orange colors indicates brush fuel (FM6); Brown indicates litter fuel (FM8); cyan color in the figure3.b indicates the mowed area; blue dots indicate unburnable area.

Field Measure Results

Fuel Loading

The average dry fine grass fuel loading measured from the Study Sites 1 was 8.98 Mg/ha (4.01 tons/acre), with minimum value of 1.00 Mg/ha (0.45 tons/acre) and maximum of 17.80 Mg/ha (7.95 tons/acre). For the Study Sites 9, the average dry fine grass fuel loading was 11.56 Mg/ha (5.16 tons/acre), with minimum value of 0 Mg/ha and maximum of 20.60 Mg/ha (9.20 tons/acre). For the Study Sites 10, due to the large portion of mowed area, the average dry fine grass fuel loading was 7.79 Mg/ha (3.48 tons/acre), with minimum value of 2.49 Mg/ha (1.11 tons/acre) and maximum of 16.19 Mg/ha (7.23 tons/acre) (measured by TFS, original data recorded in English unit). The average of mean fuel loading in the Study Site 9 and 10 was close to the mean value in the Study Site 1, therefore, the fuel loading value measured from the Study Site 1 was used as total average fuel loading value. The total measured mean grass fuel loading 8.98 Mg/ha (4.01 tons/acre) was slightly higher than the value of 6.74 Mg/ha (3.01 tons/acre) provided by Anderson (1984). The average fuel loading for top phase grass was 2.06 Mg/ha (0.92 tons/acre), and bottom phase grass was 7.88 Mg/ha (3.52 tons/acre).

The fuel loading for woody plant (fuel model 6, 8) was not sampled in this study. The data used in model was derived from a study conducted at the nearby Balcones Canyonlands National Wildlife Refuge (White, unpublished data) (Table 1). The actual woody plant fuel loading at the study site was thought to be consistent with these data, considering the similar environmental condition of the two sites.

Table 1. Field measured minimum, mean, and maximum fuel loading for each fuel model. For fuel model 6 and 8, coarse woody fuel loading (10 hour, 100 hour) also included.

Fuel Model	Fuel Type	Min (Mg/ha)	Mean(Mg/ha)	Max(Mg/ha)
FM3	1 hr	1.00	8.98	17.80
FM6	1 hr	1.14	2.08	2.84
	10 hr	0.96	1.95	3.18
	100 hr	0	0.85	3.20
	Sum	2.10	4.88	9.22
FM8	1 hr	0.16	1.23	2.42
	10 hr	0.58	1.59	3.22
	100 hr	0.25	3.38	8.60
	Sum	0.99	6.19	14.24

Fuel Moisture

In the Study Site 1, the measured relative moisture content (RMC) for grass fuel was averagely about 10%. The fuel samplings in the Study Site 9 and 10 were conducted in July summer. The sampled fuel moisture was higher than that of Study Site 1. The RMC measured for the Study Site 9 was 108% and RMC for the Study Site 10 was 89%. The difference of RMC between Study Site 9 and 10 was due to the presence of the mowed fuel area in Study Site 10 which contained higher proportion of dead grass fuels. Although without a precise measurement, the proportion of live herbaceous fuel in total fine fuel loading was assumed around 25% percent. These fuel moisture values were utilized as initial fuel moisture values for the 1-hour fuel category of the grass fuel model.

Fuel Height

The measured average fuel height of little blue stem was 1.2 meter (4 feet) in the Study Site 1, with maximum height of 1.60 meter (5.25 feet) and minimum height of 0.30 meter (1 feet). This value was greater than the average height of 0.75 meter (2.5 feet) for grass fuel type provided by Anderson 1984. For the Study Site 9, the average fuel height was similar to the Study Site 1 as 1.1 meter (3.8 feet), with measured maximum height 2.59 meter (8.5 feet). The fuel height in the Study Site 10 was smaller since most of this site was mowed before the fire. The fuel height measured for Study Site 10 was about average 0.77 meter (2.6 feet), with mowed area fuel height less than 0.46 meter (1.5 feet) and un-mowed area higher than 4 feet.

Fuel Surface Area-To-Volume Ratio

Two methods were used to measure the surface area-to-volume ratio of fuel: the water immersion technique and the leaf & stem shape simplification technique. The SAV of little bluestem result from the water immersion technique was 1345, and the result came from the second technique was around 3000. The result from water immersion technique was closer to the value offered by Anderson (1500), which indicated water immersion technique was more accurate to measure the surface area-to-volume ratio in grasslands.

Develop Fuel Map

The minimum, mean, maximum NDVI values from the three remote sensing data (Table 2) and the field measured fuel loading values (Table 1) were used to develop the regression models (Table 2). For instance, the regression equation for NDVI values from

DOQ image and the fuel loading value was: FL (Fuel Loading) =12.97*NDVI+0.84. By applying these equations on NDVI image, fuel loading image were produced. Similar regression equations were developed for each fuel model using each remote sensing data (Table 2, Graph 1).

Table 2. The minimum, mean, and maximum NDVI value from each remote sensing data for its corresponding main fuel model. The regression models developed from NDVI value and fuel loading data (Table 1) were also showed for each fuel model.

Fuel Model	NDVI	Min	Mean	Max	Regression Equation
FM 3	DOQ	0	0.20	0.57	FL=12.97*NDVI+0.84
	ASTER	0.16	0.41	0.60	FL=16.62*NDVI-2.31
	Landsat	0.38	0.56	0.74	FL=20.87*NDVI-7.60
FM 6	DOQ	0	0.29	0.53	FL=1.44*NDVI+0.51
	ASTER	0.19	0.44	0.60	FL=1.81*NDVI+0.16
	Landsat	0.42	0.62	0.75	FL=2.32*NDVI-0.48
FM 8	DOQ	0.01	0.38	0.68	FL=8.82*NDVI+0.04
	ASTER	0.27	0.51	0.60	FL=16.05*NDVI-4.20
	Landsat	0.44	0.67	0.75	FL=17.42*NDVI-7.60

Based on the regression model, sub-fuel classes for each main fuel model were determined by stratifying the fuel loading range according to its variance. Six sub-fuel classes were classified for the fuel model 3 (FM3), four sub-fuel classes for the FM6 and two sub-fuel classes for the FM8. The median values of each stratifying fuel loading range were assigned as the average fuel loading value for each sub-fuel class (Table 3).

The similar regression model method also applied on 10 hour and 100 hour fuel for FM6 and FM8 to calculation the fuel loadings for each sub-fuel class. All the assigned fuel loading values for each fuel class were input into custom fuel model file as the initial fuel loading parameters.

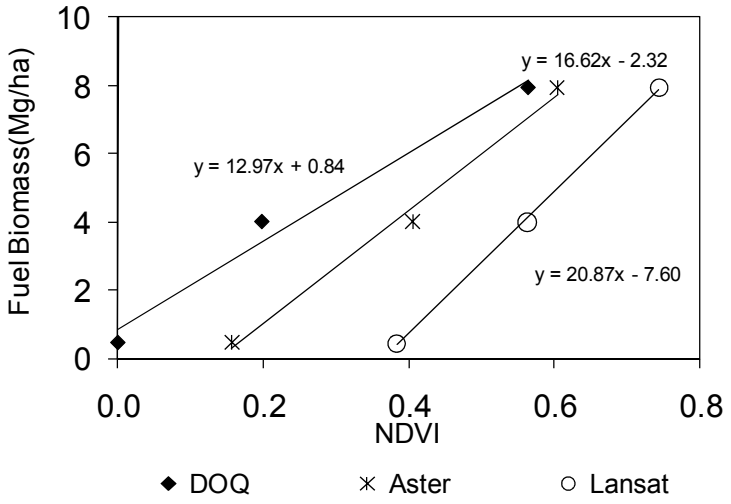

Graph 1. FM3 blue stem tall grass regression model for each remote sensing data, developed from field measured fuel loading values and NDVI values from remote sensing data. X-axis represents the NDVI value, and Y-axis represents fuel loading biomass value. The regression equations were showed on the graph.

Model Calibration Results

In custom fuel model file (.FMD), besides the fuel loading values, parameters like fuel bed depth (fuel height), surface area-to-volume ratio, and the moisture of extinction were tuned during the model calibration (Table 4). The results of calibration on the Study Site 1 showed that the best parameters for fuel model 3 (tall grass) is different with both Anderson provided values and field measured values. The modified fuel depth for grass was 1.54 feet, smaller than both Anderson's and field measured values. The modified surface area-to-volume ratio, 1550, was close to the value measured from water

immersion technique. The moisture of extinction value for grass fuel in this study was modified to be 13 other than 25 (Anderson value). The moisture extinction values for woody fuels were also modified to be 11.

Table 3. Fuel loading values ranges and assigned average fuel loading values for each Sub-Fuel class. Original data were recorded and analyzed in the unit of t/acre, and then converted to the unit of Mg/ha.

Fuel Model **3**	Sub Fuel Class	**14**	**15**	**16**	**17**	**18**	**19**
(Tall grass)	Fuel loading range	0 ---	3.4---	6.7--	10.0-	13.8-	>16.8
	(Mg/ha)	3.4	-6.7	-10	-13.5	-16.8	
	Fuel loading assigned	1.68	5.03	8.40	11.75	15.11	18
Fuel Model **6**	Sub Fuel Class	**20**	**21**	**22**	**23**		
(Post-Oak)	Fuel loading range	0----	1.68-	2.24-	>2.80		
	(Mg/ha)	1.68	-2.24	-2.80			
	Fuel loading assigned	0.85	1.97	2.50	3.10		
Fuel Model **8**	Sub Fuel Class	**24**	**25**				
(Red-Ash)	Fuel loading range	0---	>1.12				
	(Mg/ha)	1.12					
	Fuel loading assigned	0.56	1.68				

The moisture files (.FMS) used for the Study Site 1 winter burn and the Study Sites 9 and 10 summer burn was different. According to pre-fire sampling, the relative moisture of fine grass fuel in the Study Site 1 was on average 10% at the time of ignition. For the Study Site 9 and 10, the total field measured fuel moisture (including both live and dead fuel) was about 90% at the time of burn. There was no data to separate fuel moisture for dead fuel and live fuel. A value of 13% was calculated for dead fine grass

moisture assessed from recorded dry bulb temperature 32 °C (90°F) and air relative humidity (35%) using the method provided by Rothermel (1983). The moisture for live fuel used the default value (100%).

The adjustment factors were modified for different fire scenario according to the observed data. 0.6 adjustment factors were used for all grass sub-fuel classes in the Study Site 1 winter burn. And, 1.0 adjustment factors were applied on the Study Site 9 and 10 summer burn.

Table 4. Model parameters for Fuel model 3 (Tall grass) from different sources. Calibration results for other two fuel models were not showed in table.

Parameters	Anderson	Field measured	Model calibrated
Fuel depth (meter)	0.76	1.22	0.47
Fuel loading (Mg/ha)	6.74	8.98	8.96
SAV (m^{-1})	1500	1345(3000)	1550
Moisture extinction (%)	25	*not measured*	13

Simulation Results

Sub-Fuel Class vs. Main Fuel Model

The Study Site 1 fire was used to test the effect of developing finer sub-fuel classes for FARSITE simulation under grassland scenario. Overall, the sub-fuel class fuel map derived from DOQ image improved the accuracy of FARSITE modeling compared to the main fuel model fuel map.

Comparison of the simulated results of fire extent using sub-fuel class map derived from DOQ image with the results from using main fuel model map showed

differences in area burned (Figure 4.a & Figure 4.b). Visually, the variable sub-fuel class simulation had higher fidelity with the observed burn perimeter as compared to the main fuel model simulation. The simulation with only main fuel model also failed to predict fire activity at the lower right fire

Both simulations (DOQ sub-fuel classes and main fuel models) offered similar pattern of simulated time of arrival (Graph 2). There was no significant difference in time of arrival of fire prediction between using sub-fuel class map and main fuel model map. They both tended to underestimate of time of arrival, in other words, predicted higher rate of spread than it actually was (slope smaller than 1). Simulation with only main fuel model predicted higher fire spread rate.

The comparison of temperatures showed simulation use main fuel model map offered almost consistent temperature output for every data point, and simulation use sub-fuel class fuel map better revealed the heterogeneity of fire intensity at different location (Graph 3).

(a) Main Fuel Model Simulation (SS 1)

Figure 4. FARSITE simulations (continue in next page). The white lines represent simulated fire movement at each 30 minutes time step; the red bold line represents real fire perimeter. Different colors on the map represent different fuel types: green indicates grass fuel (FM3, the darker the color is, the heavier the fuel loading is); yellow to orange indicates brush fuel (FM6); Brown indicates litter fuel (FM8); cyan color in the figure 4.e,f,g indicate the mowed area; blue dots indicate unburnable area. (a), simulation ran on main fuel model map (without variable sub fuel classes) on the Study Site 1; (b), simulation ran on variable sub-fuel class derived from DOQ data on the Study Site 1; (c), simulation ran on variable sub-fuel class derived from ASTER data on the Study Site 1; (d), simulation ran on variable sub-fuel class derived from Landsat data on the Study Site 1; (e), simulation ran on variable sub-fuel class derived from DOQ data on the Study Site 9&10; (f), simulation ran on variable sub-fuel class derived from ASTER data on the Study Site 9&10; (g), simulation ran on variable sub-fuel class derived from Landsat data on the Study Site 9&10.

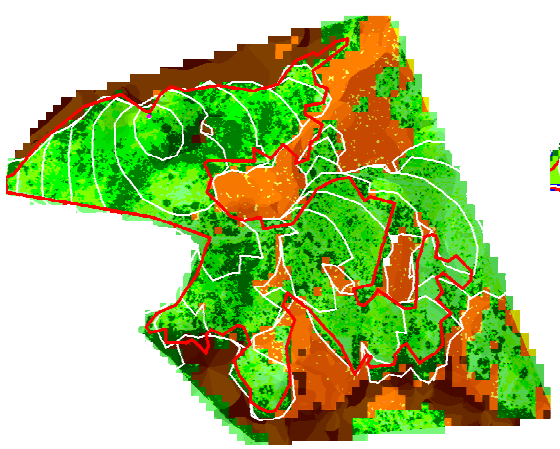

(b) DOQ Sub-Fuel Class Simulation (SS 1)

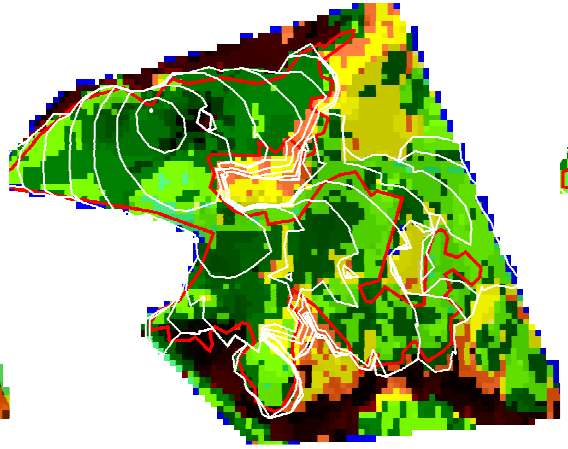

(c) ASTER Sub-Fuel Class Simulation (SS1)

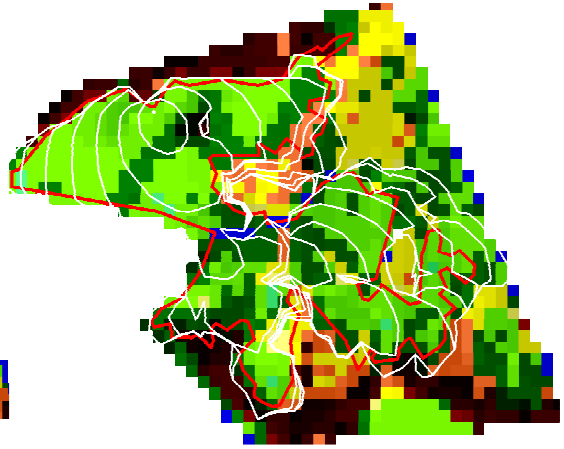

(d) Landsat Sub-Fuel Class Simulation (SS1)

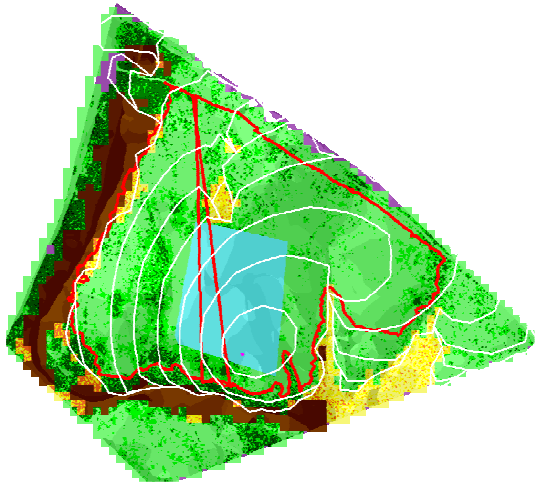

(e) DOQ Sub-Fuel Class Simulation (SS 9&10)

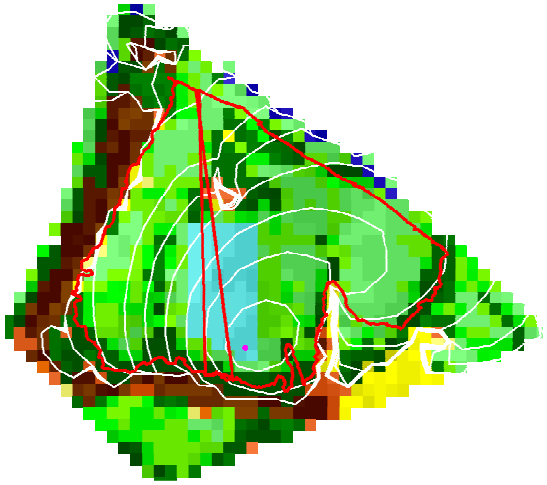

(f) ASTER Sub-Fuel Class Simulation (SS 9 &10)

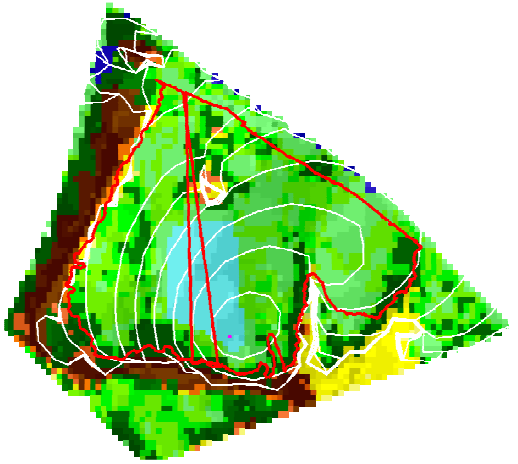

(g) Landsat Sub-Fuel Class Simulation (SS 9&

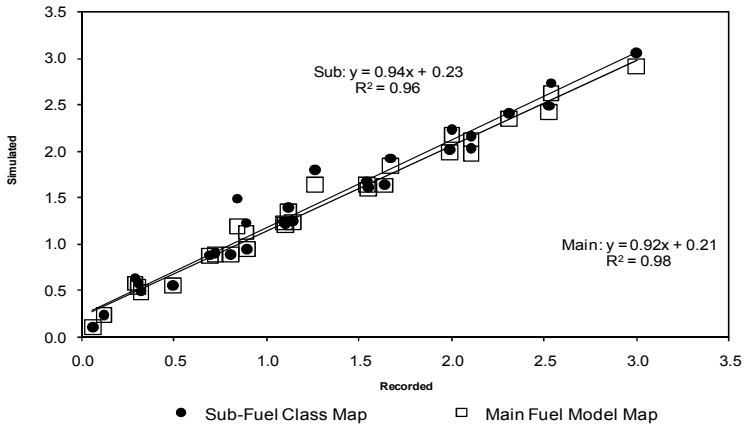

Graph 2. Plot the time of arrival of modeling results of using sub-fuel class map derived from DOQ data and using main fuel model map. X axis represented recorded time of arrival, Y axis represented simulated time of arrival. The solid line indicated the 1:1 line. Regression equation and R square were showed on the graph.

Fuel Map Scale Effect on Fire Extent:

The Study Site 9 and 10 were considered as one fire in calculating the simulated fire extent. For all simulated fires, FARSITE tended to overestimate fire extent, as compared to observed values (Table 5). Generally, there were no significant differences between the observed fires extent and all types of remote sensing data derived simulations. However, finest scale data DOQ derived simulations did offer the closest fire extent simulation results, 55 hectares in the Study Site 1 and 68 hectares in the Study Site 9 and 10. The analyses of error matrix analysis showed that the DOQ derived simulations had better overall estimate accuracies about the fire configuration and higher kappa statistics than other two remote sensing data derived simulation in both sites (Table 6). The median scale ASTER fuel map derived simulation had a better perdition results in Study Site 1 modeling than Landsat data derived simulation, but had a less perdition power in Study Site 9 and 10 simulation.

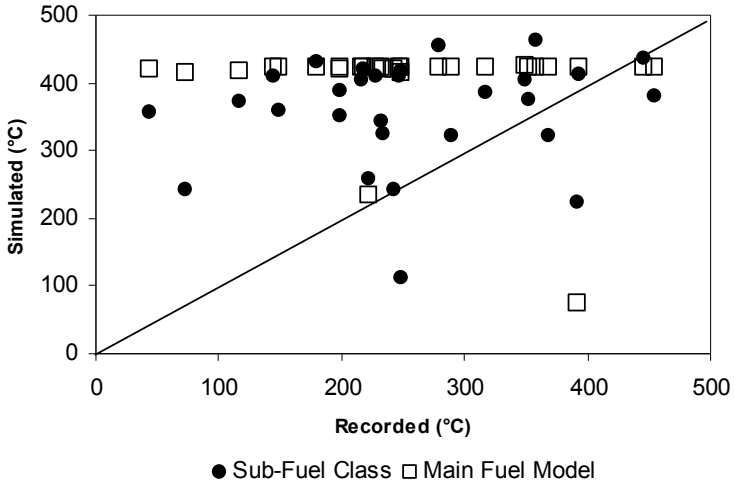

Graph 3. Plot the temperature modeling results of using sub-fuel class map derived from DOQ data and using main fuel model map. X axis represented recorded temperature, Y axis represented simulated temperature. The solid line indicated the 1:1 line.

Table 5. The fire extent comparison between observed area and simulation results using three remote sensing derived fuel maps for two prescribed burns.

Study Site	Observed (ha)	DOQ (1m) (ha)	ASTER(15m) (ha)	Landsat (30 m) (ha)
Study Site 1	42.16	54.95	59.05	60.72
Study Site 9 and 10	45.17	68.31	71.82	69.21

Table 6. Error matrix accuracy analysis, overall accuracy and kappa statistic were showed for each remote sensing derived simulation

Study Site	DOQ		ASTER		Landsat	
Study Site 1	Overall accuracy	Kappa Statistic	Overall accuracy	Kappa Statistic	Overall accuracy	Kappa Statistic
	81.4%	0.63	71.8%	0.55	71.1%	0.53
Study Site 9 and 10	Overall accuracy	Kappa Statistic	Overall accuracy	Kappa Statistic	Overall accuracy	Kappa Statistic
	78.5%	0.63	72.4%	0.59	76.1%	0.61

Fuel Map Scale Effect on Modeling Time of Arrival

The plot of simulated time of arrival versus recorded values showed that the results of all three scale simulations using different remote sensing derived fuel maps strictly follow the 1:1 line in the Study Site 1(Graph 4, a).

The plots became more scatter after applying the model on the Study Site 10 and most plots were above the 1:1 line, indicating the accuracy of model dropped (Graph 4, c). The plots also closely followed the 1:1 line in the Study Site 9 simulation, and most plots were above the 1:1 line (Graph 4, e). The standard error term was low (average 0.15) and r^2 was high (average 0.96) in the Study Site 1 simulation, which indicated high accuracy of prediction. The SEE went up higher (average 0.33) and r^2 dropped sharply (to average 0.45) after applying the model on the Study Site 10. For the Study Site 9 simulation, the SEE term slightly dropped to 0.30 compared to those from the Study Site 10, but the r^2 values were higher with an average 0.85 (Table 7).

The slopes and intercepts were compared between different scale simulations. Overall, the simulations using DOQ data (1m resolution) and ASTER data (15m resolution) yielded better result (slope close to 1, intercept close to 0) than the simulations using Landsat data (30 m resolution) in all study sites. Simulations using DOQ data offered slightly better results than ASTER data in the Study Site 1 and 10, but ASTER data did better in the Study Site 9 (Table 7).

All slope values were tested significance against 1 at the 0.05 α level. Only the slope of TOA from simulations using Landsat data (30 m resolution) was found to be significant the in the Study Site 10. All intercept values were tested significance against

0 at the 0.05 α level. Nearly all intercepts of TOA were tested as significant, except simulation using Landsat data in the Study Site 10.

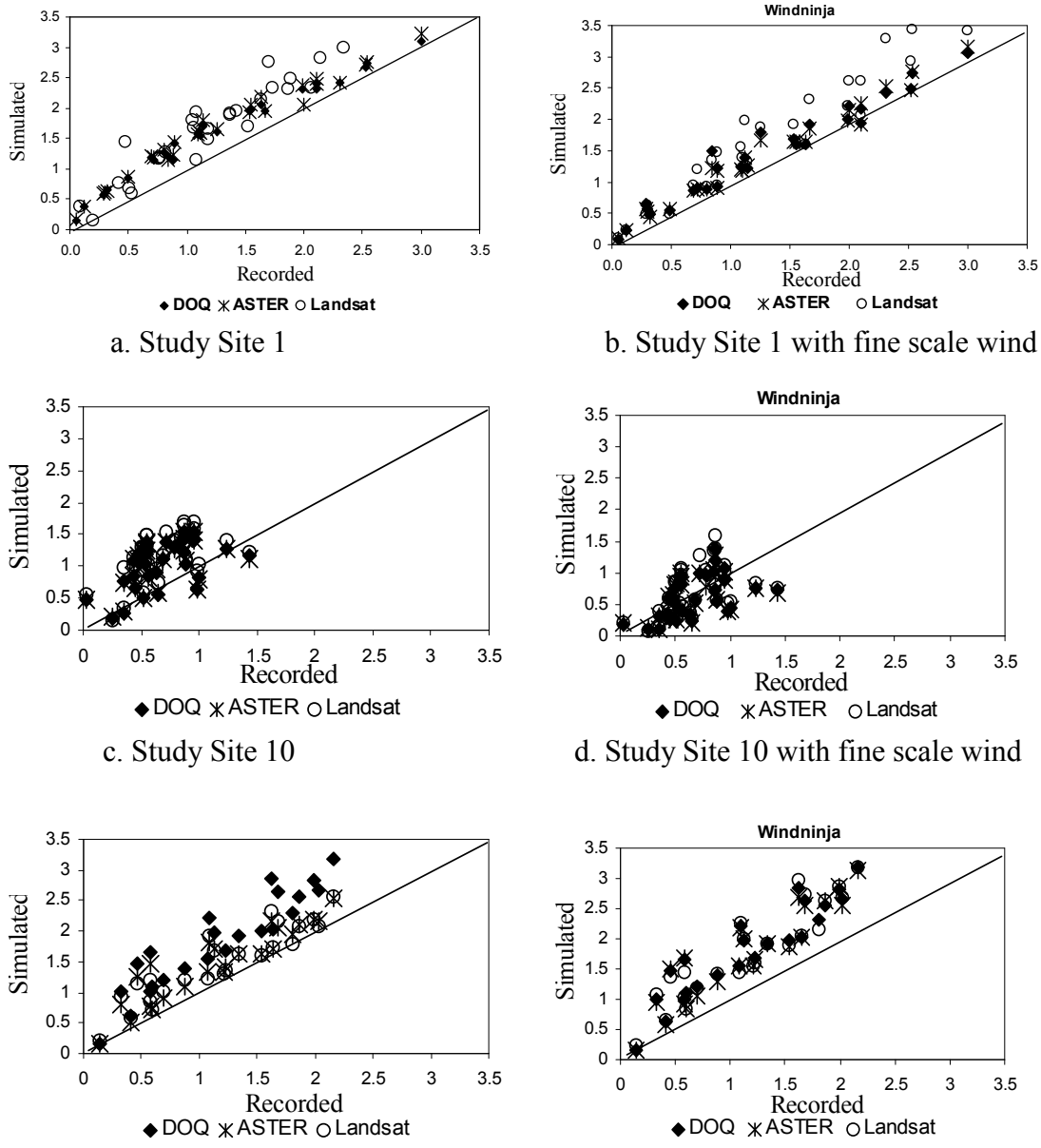

a. Study Site 1 b. Study Site 1 with fine scale wind

c. Study Site 10 d. Study Site 10 with fine scale wind

e. Study Site 9 f. Study Site 9 with fine scale wind

Graph 4. Plot the simulated value of time of arrival of fire using three remote sensing data derived fuel map versus recorded TOA values. X axis represents recorded time of arrival, Y axis represents simulated time of arrival. The solid line indicates the 1:1 line. a. Study Site 1; b. Study Site 1 with fine scale wind file; c. Study Site 10; d. Study Site 10 with fine scale wind file; e. Study Site 9; f. Study Site 9 with fine scale wind file.

Table 7. The results of the linear regression between simulated and observed time of arrival values. The * symbol indicates significant difference. a. Study Site 1; b. Study Site 1 with fine scale wind file; c. Study Site 10; d. Study Site 10 with fine scale wind file; e. Study Site 9; f. Study Site 9 with fine scale wind file.

Study Site	Data	SEE	r^2	Intercept	Slope
a. Study Site 1	DOQ	0.13	0.96	0.23*	0.94
	ASTER	0.15	0.97	0.43*	0.95
	Landsat	0.16	0.90	0.40*	0.94
b. Study Site 1 fine scale wind	DOQ	0.13	0.97	0.21*	0.95
	ASTER	0.14	0.97	0.42*	0.95
	Landsat	0.15	0.96	0.40*	0.94
c. Study Site 10	DOQ	0.33	0.43	0.47*	0.98
	ASTER	0.33	0.40	0.51*	0.92
	Landsat	0.34	0.77	0.07	2.20*
d. Study Site 10 fine scale wind	DOQ	0.31	0.51	0.05	1.08
	ASTER	0.32	0.45	0.11	1.02
	Landsat	0.41	0.72	-0.40	2.27*
e. Study Site 9	DOQ	0.30	0.86	0.47*	1.16
	ASTER	0.24	0.85	0.39*	0.93
	Landsat	0.24	0.84	0.42*	0.91
f. Study Site 9 fine scale wind	DOQ	0.29	0.92	0.42*	1.16
	ASTER	0.31	0.88	0.35*	1.19
	Landsat	0.31	0.95	0.40*	1.19

Fuel Map Scale Effect on Modeling Temperature

Comparing the calculated temperature values from simulation with the recorded temperature values, no clear linear patterns were recognized from all study sites simulations (Graph 5). The liner regression analyses were not applied on the temperature study. In the Study Site 1, plots of temperature were scatter on the graph, with ASTER data more distribute at the high simulated temperature region, Landsat data more distributed at the mid or low simulated temperature region, and DOQ data in between. The same trend was been observed in the Study Site 10 simulation, but not in the Study Site 9 simulation. The temperature data in mowed Study Site 10 simulation was more concentrated than other two simulations. In the Study Site 9, FARSITE simulated some

low temperature points that were not been recorded by dataloggers (all plot moved towards left).

Table 8. The mean temperature of data recorded values and all simulated values in all study sites.

Study Site	Recorded (°C)	DOQ (°C)	ASTER (°C)	Landsat (°C)
Study Site 1	256.6	274.4	361.2	256.9
Study Site 10	313.9	336.2	359.3	263.2
Study Site 9	402.5	297.0	248.1	298.9

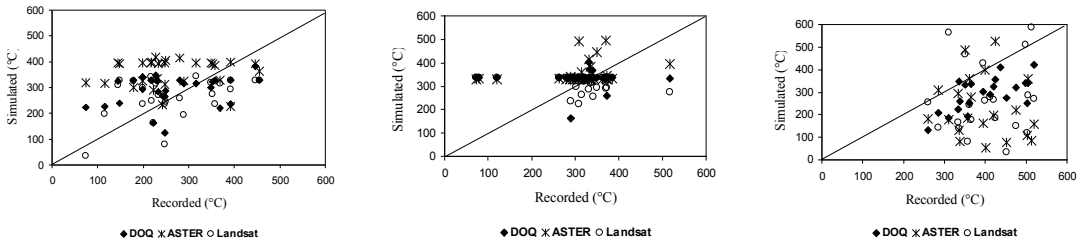

a. Study Site 1 b. Study Site 10 c. Study Site 9

Graph 5. Plot the temperature modeling results of all scale simulations. X axis represents recorded temperature, Y axis represents simulated temperature. The solid line indicates the 1:1 line. a. Study Site 1; b. Study Site 10; c. Study Site 9

Although the linear patterns of temperature were week, the mean value of simulated temperature was close to the recorded values (except in the Study Site 9) (Table 8). Generally, the ASTER data derived simulations offered the highest temperature output, and the DOQ data derived simulations had the closest temperature output as compared to the recorded values.

Scale Effect of Wind File on TOA

The WindNinja effect in the Study Site 1 was not clear (Graph 3,b), because the Study Site 1 had been well calibrated site and already with highly accurate result. However, it did help to reduce the standard error and intercept values for comparison of TOA across all scale fire simulations.

In the Study Site 10 simulation, after applying the spatially wind file, the plots tended to shift close to 1:1 line and more concrete (Graph 3,d), and the intercept moved closer to 0 and became not significant(Table 7). The r^2 increased and standard error dropped in both DOQ and ASTER derived simulations. Slopes increased in both DOQ and ASTER derived simulation after applying the spatial wind file (Table 7). In the Study Site 9, the spatial wind file also had the effect of shifting the plots closer to the 1:1 line, increasing r^2 values, and reducing the intercepts.

CHAPTER FOUR

Discussion

Accuracy of Developing Fuel Map

Three kinds of remote sensing data were used in this project to develop fuel maps which influenced the results of this study. The average NDVI value of the study sites from three remote sensing data was different with the average DOQ = 0.2, ASTER = 0.4, and Landsat ETM+ = 0.5 (Graph 6).These differences are likely due to the differences in date of acquisition of the data and caused the inconsistency in classifying sub-fuel class by only using NDVI value. However, using the regression model, the NDVI values were transferred into standardized fuel loading values and then used to stratify the main fuel model into sub-fuel class.

The accuracy of using NDVI data from three remote sensing data to analog fuel loading was questionable, since the data were taken at the different time and at least 2 years from the actual burn date. Plot the field measured fuel loading values at each data collection point with their corresponding NDVI values from three remote sensing data shows only weak positive relationship in ASTER and Landsat, and negative relationship in DOQ data (Graph 6). These caused low accuracy in developing fuel map.

The distribution of classified sub-fuel classes for FM3 in the Study Site 1 by using the regression model showed: most area was classified as median load fuel classes (like Fuel Class 16, 17) by using DOQ data; ASTER data tended to produce more heavy load fuel class (18, 19); and Landsat data was likely to favor more light load fuel class (15) (Graph 7).

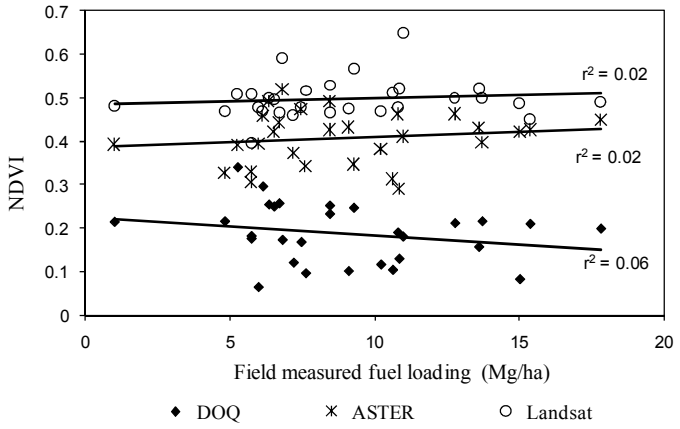

Graph 6. The scatter plot of field measured fuel loading values at each data collection point and their corresponding NDVI value from three remote sensing data. The regression line and R square values were show on the graph.

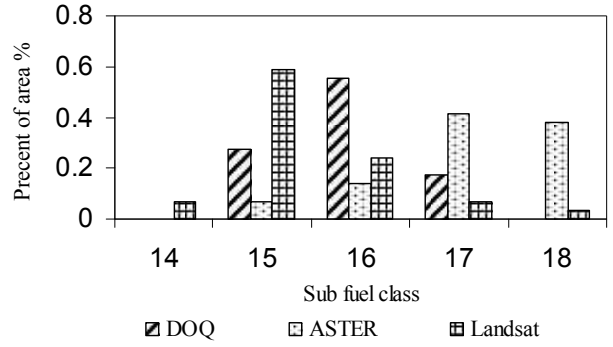

Graph 7. The distribution of classified sub fuel classes for FM3 in the Study Site 1.

Calibration of Model

Fuel Bed Depth

Calibration of model identified 0.47 meter (1.54 feet) was the best parameter of the fuel bed depth of grass for FARSITE in modeling fire in grassland scenario, which was different from both Anderson's 0.76 meter (2.5 feet) value and field measured 1.22 meter (4 feet) value. To explain this difference, a functional fuel depth was introduced in this study. Grasses like little bluestem tend to form a two-phase fuel beds: a bottom layer

was dense fuel composed of left-over fuel from previous grow seasons and new growth of small grass, and a top layer was new growth of loose grass stems with relatively large diameters (Figure 5). A functional fuel depth was calculated by weighting the height of two phases of grass according to their biomass weight.

The fuel bed depth affects the packing density of fuel, which decides the amount of air available during fire. The packing density of entire grass should be the summation of weighted packing densities of both top and bottom phase grass (Equation 13). The relative importance of visual height of each phase grass in the calculation of functional fuel height was thought to be equal to its relative importance of packing density (Equation 14). Assumed the height ratio of top and bottom phase grass fuel was 3:1 (Figure 5). According to pre-fire fuel sampling, the top and bottom phase grass fuel weight ratio was 1 : 3.87 (χ_1/χ_2 =1/3.87 in equation 13). Applied all the data into equation 14, the functional fuel depth *h* was calculated as 0.47 meter. So, the real grass fuel bed was analogous to a homogeneous distributed density fuel bed with a functional height of 0.47 meter.

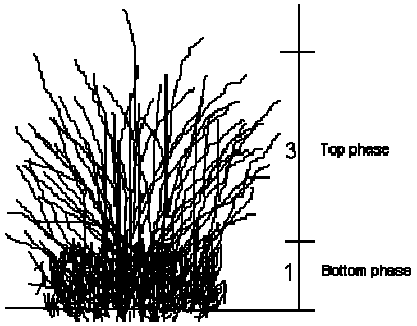

Figure 5. A demonstration of the two-phase grass bed. The height ratio between top phase and bottom phase assumed to be 3:1.

$$\frac{M_a}{d_a} = \frac{\chi_1}{\chi_1 + \chi_2}\frac{M_t}{d_t} + \frac{\chi_2}{\chi_1 + \chi_2}\frac{M_b}{d_b} \quad \text{Equation 13}$$

$$h = \frac{\chi_1}{\chi_1 + \chi_2} d_t + \frac{\chi_2}{\chi_1 + \chi_2} d_b \quad \text{Equation 14}$$

where M_a, M_t, M_b were the average, top, and bottom fuel weight; d_a, d_t, d_b were the average, top, and bottom fuel height; χ_1, χ_2 were the ratio of top and bottom fuel; h was the functional height of fuel bed.

Moisture of Extinction

Anderson gave a value of 25 for moisture extinction of fuel model 3, 6, and 8. However, this value did not work in the southern grassland ecosystem. The fire simulation running on this moisture extinction value (25) created higher spread rates and burned pass the boundary of forest line, which were not consistent with the real situation. The moisture extinction value for grass in this study was modified to be 13 to get the best simulated burn area and the time of arrival of fire. The moisture of extinction values of woody fuels were also modified to be 11 in order to keep fire out of the forest line. Due to lack of data about fire behavior in the forest area, further calibration of moisture extinction in woody fuel was impossible. The modification indicated that the southern US forest was easier to burn than the northern forest at the same moisture content level. This could due to the fuel composition difference.

Adjustment Factors

As adjustment factor value 0.6 was applied for all grass sub-fuel classes in the Study Site 1 winter burn for all simulations. This modification offered good prediction of time of arrival on the Study Site 1. However, there was a confusing factor involved here.

The major wind direction at the time of ignition was perpendicular to the major axis of Study Site 1. So, it was the flank of fire that consumed the Study Site 1 instead of the head of fire. The adjustment factor 0.6 could be contributed to the correction of the calculation of flank fire spread rate, or could be contributed to the winter scenario setting. In the Study Site 9 and 10 fire simulation, most of area was consumed by the head of fire. No adjustment factors were required to achieve good TOS results.

The difference in utilization of adjustment factors for the two burns indicated either the flank fire spread calculation in FARSITE needed to be modified, or there was something missing for FASITE to compensate for fires burning in different seasons. For the first explanation, the calculation of the flank fire spread rate primarily related to the shape of fire (length to breadth ratio, LB), which is a function of mid-flame wind speed (Anderson 1983, Finney 1998). Finney (1998) modified the original LB calculation equation (Anderson, 1983) by subtracting a constant 0.397 to fit it into the FARSITE model. It is possible that the original equation need to be further modified to fit in grasslands ecosystem and the 0.6 adjustment factor applied on the fire spread rate calculation reflected this demanded modification. Fire seemed to spread faster along the major axis of wind direction and slower at the minor axis in southern U.S grassland ecosystem, as compared to that of other landscape types. For the second explanation, by comparing the weather data of the two prescribed burns, we identified that the temperature difference (19°C in winter vs. 36 °C in summer) in there two burns might be the reason for the difference of fire spread rate, given the similar air relative humidity in these two date (28% in winter vs. 32% in summer). Clearly, hot temperature might play an important role in calculating the fire spread rate as it can lower the threshold of

ignition and facilitate the energy transfer. FARSITE simulation might have underestimated the influence of ambient temperature on the fire spread.

Simulation Results Discussion

Scale Effect of Sub-Fuel Classes

From the modeling results, it can be concluded that the inclusion of variable, site-specific sub-fuel classes in model simulation yielded more accurate fire burn perimeter estimation, more heterogeneous temperature prediction. The results confirmed the advantage to develop the custom sub-fuel classes, and showed the prediction ability of fire perimeter by FARSITE was sensitive to spatial heterogeneity at this kind of small scale grasslands simulation. The homogenized fuel map might be too coarse to reflect fine-scale variability in fire environment that keeps fire actually spreading at variable rates. Homogeneous fuel map derived model would force average fire spread rate over large areas.

The results of time of arrival showed spatial heterogeneity were not important in predicting time of arrival of fire (Graph 2). First reason, the Study Site had no major spatial heterogeneity pattern (fuel bed was mostly composed from little blue stem), so the average fire spread rate was good enough: some places fire move faster, some places fire move slower, but globally, the time of arrival of fire can be predicted by using only main fuel model map. Second, the study site was too small, the problem of model forcing average fire spread at constant rate might be clearer in a larger area.

Although the positive linear relation between recorded temperature and simulated temperature using sub-fuel class fuel map were weak, the simulation using sub-fuel class

fuel map did reveal a heterogeneous pattern of fire intensity at different location (Graph 3). The accurate temperatures at different point would be of help in fine scale post-fire ecology study.

Fuel Map Scale Effect in Modeling Fire Extent

Across all scale fuel map simulations, FARSITE slightly overestimated the fire extent. One reason was human interference activities during the prescribed burns help to un-naturally stop fire spread at the certain location. Interference of fire included pre-set black lines, fire engine suppression, and the use of bull dozers to stop fires that had escaped the prescribed burn boundaries. Some interference, like black lines and unburnable roads, were implemented into FARSITE simulation by adding un-burnable or less-burnable features on the fuel map. However, not all fire interference activates were implemented into model due to the lack of sufficient information.

In the Study Site 1 burn, there were very limited artificial fire interference been applied. Most fires went self-extinct when they came across the higher moisture content forest line. The fire went weak at the late afternoon as the air temperature dropped and relative humidity went up. All fire activities were mop-up 4 hours after the ignition. In the combine burn of the Study Site 9 and 10, a lot of suppression activities were applies to control the fire due to the concern of nearby highway traffic and the high fire danger weather at that time. Few of those were implemented into FARSITE simulation because most of the suppression activities were not recorded.

All simulations had "substantial" strength of agreement of modeling the fire configuration, as their kappa statistics were between the range of 0.61-0.80 (Landis and Koch, 1977). DOQ derived simulation had the highest overall accuracies and kappa

statistics across all scale fuel map simulations. The fine scale fuel map helped to reflect fine-scale variability in fire environment that kept fire spreading at variable rates. Detail of spatial heterogeneity that helped model determined which pixels were burned in fire offered better perdition accuracy.

ASTER data derived simulation was thought to have better perdition accuracy than Landsat data derived simulation, however, there were no clear difference in ASTER and Landsat derived simulation results. ASTER data did better in Study Site 1, while Landsat did better in the Study Site 9 and 10. The accuracy difference of fuel maps might play a role here.

Fuel Map Scale Effect on Modeling TOA

In the Study Site 1 simulation, the model showed good prediction power on simulating the fire movement across all scale fuel maps, according to the low standard error, high r^2 values, and good slope value (close to 1). The prediction power of model slightly dropped when applied the model on the Study Site 9 and substantially decreased when applied the model on the Study Site 10. Over-calibration might be a reason caused these problems. The model calibrated to fit in one area may not fit in the other area. The other reason why the model prediction power decreased in the Study Site 10 is that most of this site had been mowed before the burn and that was declared as light load fuel class (Fuel class 14) in the simulation. The homogeneous fuel map in Study Site 10 simulation failed to catch the possible spatial heterogeneity of mowed field that could affect the fire behavior.

The TOA of prescribed fire were fairly predicted by the simulations using DOQ and ASTER data derived fuel maps, whereas Landsat data derived simulation resulted in

less prediction accuracy, especially in Study Site 10 simulation. All these indicated that Landsat data (30 m resolution) did not suitable to be used to develop fuel map in small scale grassland fire modeling. The high variance of results between Study Site 9 and 10 simulation using Landsat data indicated the Landsat data was unreliable. It is thought that the cell resolution of Landsat data was too coarse to catch the necessary spatial information for fire model. Fire movement across grasslands can be affect by fuel type changes (tree, shrub patch). Usually, various patch sizes within small grassland area were less than 900 m^2 (the pixel cell size of Landsat data) (observed from field). So, the Landsat data (30 meter cell resolution) couldn't catch enough patch information in the heterogeneous southern U.S grasslands landscape for FARSITE to simulate fire movement. The 30-m raster grids products from the Landsat data dependent LANDFIRE project need to be adjusted by local use (Rollins, 2009). From above results, clearly, finer scale data and information were need when applying the LANDFIRE products in the southern U.S grasslands ecosystem.

Between simulation using DOQ or ASTER data, there were no significantly different affect for FARSITE simulation using either data. The DOQ seemed worked better in the Study Site 1 and 10, while ASTER data worked better in the Study Site 9.The plot graph of remote sensing derived NDVI and measured fuel loading at each data collection point showed, although the relationships were weak, that the ASTER data had the highest accuracy in predicting the fuel (positive relationship, high r^2 value) and the DOQ had the worst accuracy on predicting fuel (negative relationship) (Graph 6). These can be used to partially explain why ASTER data derived simulation had similar prediction power on TOA as DOQ did. It was fair to predict that, with more accurate

data, simulation derived from DOQ might offer better prediction power than ASTER would.

The simulation derived from DOQ data mostly offered better prediction of intercept values. Average intercept values for all simulation was around 0.4, which indicated FARSITE had about 24 minutes delay (0.4*60=24) at the beginning of simulating fire.

Fuel Map Scale Effect in Modeling Temperature

The reason that FARSITE model did not "work" in modeling the temperature of fire might include several aspects. First, the accuracy of the developed fuel maps was questionable. Annual and seasonal variation of fuel loading, fuel type change can greatly affect the simulated reaction intensity (used to calculate temperature) results (Graph 6). So, an accurate fuel map was critical in modeling the fire temperature. Secondly, the transfer of reaction intensity to temperature may not be as straight forward as the blackbody Stefan-Boltzmann law indicated. The results of simulated reaction intensity were an average value for each pixel, while the temperature recorded by fire datalogger only represented the temperature change at its sensor's nip. So, the real relationship between temperature data recorded by fire dataloggers and the simulated fire reaction intensity was unclear. Last but not least, not all energy released as radiance heat, some was used to vaporize the moisture of fuels for instance.

The different distribution pattern of temperature plots for each remote sensing data on the scatter plot (Graph 5) can be attributed for the different distribution of fuel class derived from each remote sensing data (Graph 7). ASTER data derived simulation tended to offer higher temperature, and Landsat data were likely yielded lower

temperature output. Summer burns (Study Site 9 and 10) was more severe than winter burn (Study Site 1), as most recorded temperatures were above 200 ^{o}C (Graph 5, b,c).

Although the distribution pattern of simulated temperatures and recorded temperatures was not clear, the average temperature can be used as an indicator of modeling fire. In all simulations, generally speaking, DOQ derived simulations offered the most accurate temperature prediction, which indicated fine scale fuel map had an advantage in predicting the average temperature values. The mean temperatures also contained the ecological information about post grassland fire ecology. The average temperature yielded by fire can be used to predict what kind of vegetation seed bank could survival from grasslands fire. The different winter and summer fire average temperatures also offered information about the different impact of winter and summer fire. Summer fire yielded higher mean temperatures and tended to penetrate to deeper soil to affect seed bank and underground vegetative parts. So, generally, summer burn would favor those species whose seeds were buried deeper or more tolerant to high temperature, those species with thicker bark, as well as those species with high reproductive ability of their underground vegetative parts.

Scale Effect of Input Wind File

The wind is the most important factor affecting the change of fire behavior. The concentration of plots (graph 4. b, d, f) and the change of standard error and r^2 showed that the applying of the spatial variant wind file created by WindNinja software on the FARSITE modeling improved the precision of simulated time of arrival, as compared to using the hourly average wind data (from RAWS). The pattern was especially clear in

the Study Site 10 modeling. And, it seems the spatial variant wind file had more effect on DOQ derived simulations.

The intercept changes in the Study Site 10 simulation after applying the spatial wind file showed that fine scale wind pattern can help model to correct initial fire spread simulation (move early plot closer to 1:1 line). It can be predicted fine scale wind information was important in the initial fire simulation.

The reason why spatial wind file didn't have clear impact in the Study Site 9 simulation was that the topographic feature in this study site was relatively homogeneous (nearly flat) as compared to Study Site 10 that had a small elevation lift from west to east. So, it could be predicted that spatial wind pattern information would be more useful in fire simulation on a highly variable terrain.

The spatial wind file created by WindNinja software applied on the FARSITE modeling improved the precision of time of arrival prediction, especially at the initial stage of fire ignition simulation. The wind is the most important factor affecting the change of fire behavior. Conducting a fire simulation on a highly variable terrain, fine scale wind files should be incorporated in simulation.

CHAPTER FIVE

Conclusion

Both prescribed fire conducted on the Study Site 1 and the Study Site 9 and 10 were not proceeding according to the prescribed plan. Clearly, more knowledge about fire in the southern U.S. grasslands ecosystem was needed. FARSITE model can be used to simulate fire behavior but requires modification to fit in the southern U.S. grasslands.

Field sampling offered data to modified parameters for FARSITE in the grassland scenario. The fuel loading, the surface area-to-volume ratio, the fuel bed depth, the moisture extinction values all needed to be calibrated before input into final FARSITE simulation. In this study, the fuel loading and the surface area-to-volume ratio was similar with reference data with small modification. A functional fuel bed depth was introduced to explain the modified fuel bed depth in grasslands. The moisture extinction values were discovered lower than the reference data, indicating southern grassland fuel was more flammable. Adjustment factors were used to tune the model in different burn scenarios, 0.6 for winter burn and 1 for summer burn. Different initial moisture inputs were also used for the summer and winter fire simulation.

From the simulations, it was confirmed that main fuel models were not enough to model small scale grasslands fire. FARSITE simulations on grasslands were encouraged to involve developing sub-fuel class and include more detail information in fuel map. Inclusion of variable, site-specific sub-fuel classes in model simulation yielded more accurate fire burn perimeter estimation, more heterogeneous temperature prediction.

Use three different scale remote sensing data to develop fuel maps for FARSITE simulation revealed the scale dependency of the model to simulate fire extent, time of arrival, and the temperature. For the modeling of fire extent, DOQ derived simulations had the highest overall accuracies and kappa statistics across all scale fuel map simulations. Finer scale data and information other than 30-m Landsat data were need when applying the LANDFIRE products in the southern U.S grasslands ecosystem.

For the modeling of time of arrival, Landsat data were identified not suitable for the model. No significant differences were found between results from DOQ data and ASTER derived simulations. However, DOQ data was encouraged to used because, even with the most corrupt data among all three remote sensing data (Graph 6), DOQ derived simulation still be able to offer the results as good as ASTER did. This indicated the DOQ data offered fine scale detail to catch the information of fuel patches, which might play an important role in affecting fire movement across the landscape. The average 24 minutes delay of FARSITE model results at the initial stage indicated the inadequate accuracy of model to simulation fire behavior at the ignition stage. Time of arrival of fire tells when the fire moves to certain location. It is a useful indictor, especially for fire management personnel like wild fire fighters, to predict fire movement and to make the plan to fight fire. Most of slopes of time of arrival were less than 1, which was good because the simulated fire moved faster than the real one would give more time for people to react.

For the modeling of temperature, the FARSITE model didn't offered a good prediction of fire temperature. However, from the temperature plots distribution pattern, it can be identified that fine scale fuel map had an advantage in predicting temperature

values. Besides, DOQ derived simulations offered the most accurate average temperature prediction. The average temperature yielded by fire can be used to predict the overall impact of fire on the local soil seed bank and to predict the post fire ecological succession on the area. For example, people in Camp Swift were trying to use prescribed burn to eliminate certain vegetation, like mustang grape. The simulated average 400 °C fire offered the information that prescribed burn would be hot enough to remove mustang grape. The different winter and summer fire average temperatures also showed the different impact of winter and summer fire. For example, a winter burn with low surface temperatures and high biomass consumption in grassland may increase woody plant emergence from root sprouting. So, to suppress the woody plant, summer burn will be encouraged.

The modeling environment can propose the abiotic setting, but requires further biotic sampling and monitoring. Because, from these study, it can be told that biotic setting plays an important role in the fine scale fire simulation. The fuel condition, configuration, type change, and their energy attributes affect certain scale fire behavior modeling in the southern US grassland ecosystem.

REFERENCES

Albini, F.A. 1982. The variability of wind-aided free-burning fires. Comb. Sci. Tech. 31:303-311.

Anderson, H.E. 1970. Forest fuel ignitability. Fire Technology 6(4): 312-319

Anderson, H. E. 1982. Aids to determining fuel models for estimating fire behavior. USDA Forest Service General Technical Report INT-122, 22p.

Anderson, H.E. 1983. Predicting wind-driven wildland fire size and shape. USDA For. Serv. Res. Pap. INT-305.

Avaklan, A.J., and Wermund, E.G. 1993. Physical environment of Camp Swift Military Reservation, Bastrop County, Texas: Baseline information for National Guard Land Condition-Trend analysis program

Bean, W.T., Sanderson, E. W., 2008. Using a spatially explicit ecological model to test scenarios of fire use by Native Americans: An example from the Harlem Plains, New York, NY. Ecological Modelling 211 pp.301–308

Chandler, C., Cheney, P., Thomas, P., Trabaud, L. and Williams, D., 1983. Fire in Forestry. Vol I: Forest fire behavior and effects. John Wiley & Sons, New Your.

Collins, B.D., Stephens, S.L. 2007. Managing natural wildfires in Sierra Nevada wilderness areas. Front. Ecol. Environ. 5(10), 523-527

Congalton, R.G., Green, K. 1999. Assessing the Accuracy of Remotely Sensed Data: Principles and Practices, Lewis Publishers, New York, NY

Conover W.J. 1971. Practical Nonparametric Statistics, John Wiley & Sons, New York (1971).

Dasgupta, S. Qu, J.J., Hao, X., Bhoi, S. 2006. Evaluating remotely sensed live fuel moisture estimations for fire behavior predictions in Georgia, USA. Remote Sensing of Environment, Vol. 108, Issue 2, pp. 138-150

Diamond, D.D., Smeins, F.E., 1985. Composition, Classification, and Species Response Patterns of Remnant Tallgrass Prairies in Texas. American Midland Naturalist, Vol. 113, No. 2, pp. 294-308

Fernandes, P.M., Rego, F.C., 1998. A new method to estimate fuel surface area-to-volume ratio using water immersion. Int. J. Wildland Fire 8(2):59-66

Finney, M.A., 1993. Modeling the spread and behavior of prescribed natural fires. Presented at the 12th Conference on Fire and Forest Meteorology, Jekyll Island, Georgia, October 26–28, 1993, pp. 138–143.

Finney, M.A., 1996. FARSITE: Fire Area Simulator, ver. 3.0. Systems for Environmental Management, Missoula, Montana.

Finney, M.A., 1998: FARSITE: Fire Area Simulator—model development and evaluation. Res. Pap. RMRS-RP-4. Ogden, UT, USDA Forest Service Rocky Mountain Research Station. 47 p.

Finney, M.A., Ryan, K.C., 1995. Use of the FARSITE fire growth model for fire prediction in the U.S. national parks. Presented at the International Emergency Management and Engineering Conference. Nice, France, The International Emergency Management and Engineering Society, pp. 183–189.

Grant, W. E., Hamilton, W.T., Quintanilla E., 1999. Sustainability of agroecosystems in semi-arid grasslands: simulated management of woody vegetation in the Rio Grande Plains of southern Texas and northeastern Mexico. Ecological Modeling Volume 124, Issue 1, pp. 29-42

Grace, J.B., Allain, L.K., Baldwin, H.Q., Billock, A.G., Eddlemanm, W.R., Given, A.M., Jeske, C.W., and Moss, R. 2005. Effects of prescribed fire in the Coastal Prairies of Texas. Texas: USGS Open File Report 2005-1287.

Habselka, C.W., Drawe, D.L., Ruthven, D.C., 2007. Management of South Texas Shrublands with prescribed fire. USDA Forest Service RMRS-P-47.

Hibbard, K.A., Schimel, D.S., Archer, S., Ojima, D.S. and Parton, W., 2003. Grassland to woodland transitions: integrating changes in landscape structure and biogeochemistry. Ecological Applications:911-926.13.

Heyerdahl, E.K., Miller, R.F., Parsons, R.A., 2006. History of fire and Douglas-fir establishment in a savanna and sagebrush-grassland mosaic, southwestern Montana, USA. Forest ecology and management. 230(1-3): 107-118

Hessburg, P.F., Agee, J.K. and Franklin, J.F., 2005. Dry forests and wildland fires of the inland Northwest USA: Contrasting the landscape ecology of the pre-settlement and modern eras. Forest Ecology and Management Relative Risk Assessments for Decision -Making Related To Uncharacteristic Wildfire, 211(1-2): 117-139.

Jensen, J.R., 2000. Remote sensing of the environment. Prentice Hall, NY.

Keane, R.E., Mincemoyer, S.A., Schmidt, K.M., Long, D.G., Garner, J.L., 2000. Mapping vegetation and fuels for fire management on the Gila National Forest Complex, New Mexico. General Technical Report RMRS-46-CD. USDA Forest Service, Rocky Mountain Research Station, Missoula, MT.

KeaneA, R.E., Burgan, R. and Wagtendonk, J. van. 2001. Mapping wildland fuels for fire management across multiple scales: Integrating remote sensing, GIS, and biophysical modeling. International Journal of Wildland Fire, 10, 301–319

Landis, J.R., Koch, G. G. 1977. The measurement of observer agressment for categorical data, Biometrics, Vol. 33, No. 1 (Mar., 1977), pp. 159-174

Levin, S.A., 1992. The Problem of Pattern and Scale in Ecology: The Robert H. MacArthur Award Lecture. Ecology, 73(6): 1943-1967.

Miller, J.D. and Yool, S.R., 2002. Modeling fire in semi-desert grassland/oak woodland: the spatial implications. Ecological Modelling, 153(3): 229-245.

Miller C., and Urban, D.L., 1999. A model of surface fire, climate and forest pattern in the Sierra Nevada, California. Ecol. Model. **114**, pp. 113–135.

Morgan, P., Hardy, C. C., Swetnam, T. W., Rollins, M. G., Long, D.G. 2001. Mapping fire regimes across time and space: understanding coarse and fine-scale fire patterns. International Journal of Wildland Fire, 10, 329-342

O'Neill, R.V. 1988. Hierarchy theory and global change. In: Rosswell, T., Woddmansee, R.G. & Risser, P.G. Scales and Global change, pp. 29-45. Wiley, New York, NY.

Pitman, A.J., Narisma, G.T., McAneney, J., 2007. The impact of climate change on the risk of forest and grassland fires in Australia. Climatic Change 84: 383-401

Pyne S.J., Andrews P.L. and Laven, R.D., 1996. Introduction to Wildland Fire, John Wiley and Sons, New York (1996) pp. 769

Rollins, Matthew G., Morgan, P., Swetnam, T., 2002. Landscape-scale controls over 20th century fire occurrence in two large Rocky Mountain (USA) wilderness areas. Landscape Ecology 17: 539-556, 2002.

Rollins, Matthew G., Keane, Robert E., Parsons, Russell A. 2004. Mapping fuels and fire regimes using remote sensing, ecosystem simulation, and gradient modeling. Ecological Applications, 14(1), pp. 75-95

Rothermel, R.C. 1972. A mathematical model for predicting fire spread in wildland fuels. USDA For. Serv. Res. Pap. INT-115.

Rothermel, R.C., Deeming, J.E., 1980. Measuring and interpreting fire behavior for correlation with fire effects. General Tech. Rept., USDA, Forest Serv., INT-93:1-4

Ruthven, D.C., Synatzske, D.R., 2002. Response of herbaceous vegetation to summer fire in the western South Texas Plains. Texas J. SCI. Vol.54, Iss.3, pp.195(16)

Running, S.W., 2006. CLIMATE CHANGE: Is Global Warming Causing More, Larger Wildfires? 10.1126/science.1130370. Science, 313(5789): 927-928.

Smith, A. M.S., Wooster, M. J., Drake, N. A., Dipotso, F. M., Falkowski, M. J., Hudak, A. T., 2005. Testing the potential of multi-spectral remote sensing for retrospectively estimating fire severity in African savannahs. Remote sensing of environment. 97(1): 92-115

Stratton, R.D. 2004. Assessing the effectiveness of landscape fuel treatments on fire growth and behavior. Journal of Forestry October/Novermber pp. 32-40.

Wells, P.V. 1966. Woodlands and Grasslands in the Great Plains. Ecology, vol47, No. 1, pp.171-172

Wessman C. A., Bateson, C.A., Benning, T.L., 1997. Detecting fire and grazing patterns in tall grass prairie using spectral mixture analysis. Ecological Application, 7(2), pp.493-511

White, J.D. and Running, S.W., Nov., 1994. Testing Scale Dependent Assumptions in Regional Ecosystem Simulations. Journal of Vegetation Science, 5(5): 687-702.

White, J.D., Gutzwiller, K.J., Barrow, W.C., Randall, L.J. and Swint, P. 2008. Modeling mechanisms of vegetation change due to fire in a semi-arid ecosystem. Ecological Modelling 214 (2008)181-200

Whitlock, C., Moreno, P.I. and Bartlein, P., 2007. Climatic controls of Holocene fire patterns in southern South America. Quaternary Research, 68(1): 28-36.

Whelan, R.J. 1995. The ecology of fire. Cambridge Studies in Ecology

Wright, H.A., Bailey, A.W., 1982. Fire ecology: United States and Southern Canada. John Wiley and Sons, New York, NY.